A NOVEL TRAIL TO NEUROINFLAMMATION: COMMON CLUES TO NEURODEGENERATIVE DISORDERS

G. DI BENEDETTO[1], O.VALERIO[1], G. TAFET[2], N. RONSISVALLE[1], R. DI MAURO[1], G. FUCCIO SANZÀ[1], G.R.M. SACCANI-JOTTI[3], R. BERNARDINI[1] and G. CANTARELLA[1]

[1]Department of Biomedical and Biotechnological Sciences, Section of Pharmacology, University of Catania School of Medicine, Catania, Italy; [2]Departimiento de Neurociencias y Psiquiatria, Maimonides University, Buenos Aires, Argentina; [3]Department of Biomedical, Biotechnological and Translational Sciences, Faculty of Medicine, University of Parma, Italy

Convincing evidence supports the pathophysiologic relevance of inflammatory mediators expressed by injured cells during neurodegenerative processes. Among these, proapoptotic/proinflammatory cytokines belonging to the TNF family and their receptors are regarded as sustainers of the accelerated cell death rate occurring in neurodegenerative processes related to various CNS disorders. In this line, tumor necrosis factor-related apoptosis inducing ligand, or TRAIL, a proapoptotic cytokine which acts through its two DR4 and DR5 death receptors, has been shown to potently mediate prominent neuronal loss in conditions of neuronal injury, such as amyloid accumulation, brain ischemia, and traumatic spinal cord injury. In fact, these conditions share increased TRAIL, DR4 and DR5 expression, associated with activation of caspases, augmented neuronal death rate, gliosis, and overexpression of an array of proinflammatory mediators. Furthermore, high TRAIL expression is proportional to functional decline, which eventually brings about, for example, severe impairment of related functions. In animal models of neurodegeneration, immunoneutralization of TRAIL by means of a monoclonal antibody results in significant rescue of injured neurons from death. In fact, molecular, tissue, and functional parameters show dramatic improvement in individuals receiving anti-TRAIL treatment. In synthesis, TRAIL is a detrimental factor activated by damaged neurons. TRAIL efficiently sets into motion redundant neurodegeneration–related cell death processes, and its neutralization implies either significant attenuation or abrogation of phenomena typical of neurodegeneration. For these reasons, the TRAIL system, which represents a common clue to many neurodegenerative processes, should be regarded as a potential target for efficacious, innovative therapeutic strategy of neurodegenerative disorders, aimed to restrain overshooting neuroinflammation and its detrimental consequences.

In 1995 and 1996, Wiley and Pitti, independently of each other, discovered a protein that was able to rapidly induce apoptosis. Such protein was named TNF-related apoptosis-inducing ligand (TRAIL), or Apo2L, respectively because of its high homology to other members of the TNF family, and its close relation to Fas/Apo-1 ligand. TRAIL consists of respectively 281 and 291 amino acids in the human and murine

Key words: cytokines, neurodegenerative disorders, immunotherapy

Corresponding author: Renato Bernardini MD,
Department of Biomedical and Biotechniological Sciences,
Section of Pharmacology,
University of Catania Medical School,
Viale Andrea Doria, 6
95125 Catania, Italy
e-mail: bernardi@unict.it

2279-5855 (2015)

DISCLOSURE: ALL AUTHORS REPORT NO CONFLICTS OF INTEREST RELEVANT TO THIS ARTICLE.

forms, which share 65 percent identity (Wiley et al, 1995; Pitti et al, 1996). Like other members of the TNF ligand family, TRAIL is expressed as a type II transmembrane protein and is released from the cell membrane after cleavage by metalloproteinases, yielding soluble TRAIL. The C-terminus of TRAIL can be processed proteolytically to form a soluble ligand. The extracellular domain encompasses two antiparallel beta-pleated sheets that form a beta sandwich and 12–16 aminoacid N-terminal insertion loops. Active TRAIL forms a homotrimer that binds three receptor molecules at the interface between two of its subunits (Almasan and Ashkenazi, 2003). A Zn^{++} atom bound by cysteines in the trimeric ligand is essential for optimal biological activity (Hymowitz et al, 2000; Bodmer et al, 2000).

Both the full-length and the soluble version of TRAIL induce apoptosis in various human cancer cell lines, and it was initially believed not to affect normal cells (Wiley et al, 1995). Various human tissues and multiple cell types express TRAIL, including lung, liver, thymus, placenta, ovary, small and large intestine, and heart. Structurally, TRAIL comprises short intracellular, transmembrane, and large extracellular regions (Cummins et al, 2004). Initially, research was focused on the potential use of recombinant TRAIL as an anti-tumour agent, as well as in functions of endogenous TRAIL in anti-tumour immunity (Bouralexis et al, 2005). However, later reports demonstrated proapoptotic effects of TRAIL also on non-transformed cells, including neurons (Nitsch et al, 2000) and hepatocytes (Jo et al, 2000).

Interestingly, despite increased expression of TRAIL being described in ischaemic mouse brain (Martin-Villalba et al, 1999), there was no evidence for its presence in the adult human brain. Nevertheless, death-domain and TRAIL decoy receptors are widely distributed in the human CNS (Nitsch et al, 2000).

TRAIL AND ITS RECEPTORS

TRAIL interacts with five distinct receptors encoded by separate genes but share high sequence homology in their extracellular domains. In humans, TRAIL binds to five members of the TNF-α receptor superfamily. Of these, death receptor-4 (DR4) and death receptor-5 (DR5) are type I transmembrane proteins equipped with an intracellular death domain (DD) (LeBlanc and Ashkenazi, 2003). In contrast, mice have only one TRAIL receptor with death signalling capacity, mDR5 (Wu et al, 1999). DR4 and DR5 contain an intracellular death domain defined as apoptosis-inducing receptor (Fig. 1).

Other two TRAIL-binding receptors are the membrane-bound decoy receptor (DcR) 1 and 2. DcR1 entirely lacks a cytoplasmic domain, whereas DcR2 has a nonfunctional truncated death domain. Because of these features, DcRs cannot trigger apoptosis and, instead, inhibit TRAIL signaling. The fifth receptor, osteoprotegerin (OPG), binds to TRAIL with very low affinity (Gaur et al, 2003), and it regulates osteoclastogenesis by binding receptor activator of nuclear-factor kB ligand (RANKL) (Held and Schulze-Osthoff, 2001).

The biologically active form of TRAIL is a homotrimer that triggers apoptosis through bond with DR4 or DR5, thus leading to subsequent assembly death-inducing signalling complex (DISC) (Walczak and Haas, 2008). This is the first step of apoptosis induction by TRAIL. The response to TRAIL may be elicited through two distinct modalities, the extrinsic and the intrinsic pathway (Huang et al, 2005).

The extrinsic apoptotic pathway is characterized by the formation of the DISC complex. Then, Fas-associated death domain (FADD) translocates to the DISC and there recruits procaspases 8 and 10; in particular, FADD acts as a bridge between DISC and the pro-domain of the caspase 8 and 10, that are subsequently activated and released into the cytosol. The formation of a mature form of caspase 8 leads to activation of downstream effector caspases such as caspases 3, 6 and 7 (Fulda and Debatin, 2004), finally leading to the cleavage of target proteins, fragmentation of DNA and cell death.

By contrast, the intrinsic apoptotic pathway is set into motion through different stress signals that damage mitochondria. It is characterized by the translocation of pro-apoptotic members of the Bcl-2 family to the mitochondria, like Bax and Bak, leading to loss of transmembrane potential, release into the cytosol of cytochrome *c* (cyto*c*) and other mitochondrial factors, such as second mitochondria-derived activator of caspases/direct IAP binding protein with low pI (Smac/DIABLO), apoptosis inducing factor (AIF), and endonuclease G (Duiker

et al, 2006). In the cytosol, cyto*c*bindsapoptotic protease activating factor 1 (Apaf-1) and pro-caspase 9, leading to the formation of the apoptosome. Cyto*c* and Apaf-1 activate caspase-9 with subsequent activation of effector caspases 3, 6 and 7 (Falschlehner et al, 2009). Smac/DIABLO counteracts the function of X-linked inhibitor of apoptosis protein (XIAP), thereby allowing activation of caspases 3, 7 and 9 (Shi, 2004).

Both the intrinsic and extrinsic pathways can direct the apoptotic signalling cascade, and are connected via the BH3-domain-only subfamily protein, Bid. After cleavage to truncated Bid by active caspase 8 or active caspase 10, tBid is translocated to the mitochondria, conducting to the activation of Bax or Bak and inducing release from the mitochondria cyto*c* and other pro-apoptotic proteins (Waterhouse et al, 2002).

In addition, various other protein kinases such as mitogen-activated protein kinase (MAPK), extracellular signal-regulated kinase (ERK), c-Jun N-terminal kinase (JNK), and p38, along with the transcription factor NF-kB, can regulate the apoptotic pathways activated by TRAIL (Bhardwaj et al, 2003).

Apart from apoptosis, results from *in vitro* and *in vivo* experiments have revealed that TRAIL can induce cell death through nonapoptotic mechanisms, such as necrosis (Guo et al, 2005; Voigt et al, 2014).

TRAIL AND ITS RECIPROCAL ROLE WITH OTHER CYTOKINES OF THE TNF SUPERFAMILY

The TNF superfamily consists of a wide array of ligands and receptors. In fact, over twenty ligands and thirty receptors have been identified in humans, in addition to three more receptors in mice. The first members to be identified are TNF-α and TNF-β (Aukrust et al, 2011).

TNF superfamily ligands and receptors are key molecules in physiological developmental processes involving apoptosis, survival, differentiation and proliferation of cells, regulation of immune cell functions and additional cell type-specific responses. Therefore, they underlie important functions in human disorders like autoimmune diseases and cancer. Mutations in both ligands and receptors, for example TNFR1, CD95 or CD95L, can be the cause of abnormalities. In particular, humans with mutations in TNFRSF1A encoding TNFR1, manifest episodes of fever and severe localized inflammation, called TNFR1-associated periodic syndromes (TRAPS) (Negm et al, 2014).

Most TNF ligands are expressed on cells involved in the immune system, such as B-cells, T-cells, NK cells, monocytes and dendritic cells, whereas the TNF receptors are expressed by cells with both hematopoieticand non-hematopoietic origins. The majority of TNF ligands are type II transmembrane glycoprotein, having a long extracellular domain and a short cytoplasmic region. In particular, the ligands consist of a varying lengthstalk which joins the transmembrane domain with the core region containing the TNF homology domain (THD) or, in other words, the hallmark structure of TNF family ligands. The THD is an anti-parallel beta-pleated sheet sandwich with a "jelly-roll" topology. The extracellular domains can be cleaved by specific metalloproteinases to produce soluble cytokines. In general, cleaved or non-cleaved ligands operate as non-covalent homotrimers except for lymphotoxin beta and BAFF (B Cell Activating Factor). The lymphotoxin beta specifically form sheterotrimers with TNF-β and the BAFF forms heterotrimers with APRIL (A Proliferation-inducing Ligand). In general, TNF ligands bind to single receptor, but for example TRAIL bind five different receptors (Bodmer et al, 2002). Receptors for TNF superfamily ligands are oligomeric type I or type III transmembrane proteins. TNF receptors are classified into three different groups. The first group includes TNFR2, CD40, TACI, GITR, EDAR, and XEDAR. They contain TNF receptor-associated factors (TRAF)-interacting motif (TIM) in cytoplasmic tails. (David et al, 2002). Ligands binding to TIM containing TNF receptors recruit TRAF family members and start up cellular signaling pathways involving activation of a nuclear factor-kB (NF-kB), p38, Jun N-terminal kinase (JNK), extracellular signal regulated kinase (ERK) (Darnay et al, 1999). The second group of receptors (i.e. CD95, DR3, DR4, DR5, DR6) contain intracellular death domains (DDs) that recruit caspase-interacting proteins following ligand binding to start the extrinsic pathway of caspase activation. They are characterized by the following features:

extracellular aminoterminal cysteine-rich domanis (CRDs), which contributes to ligand specificity; pre-association of the receptor to the plasma membrane; death domain, located in the cytoplasmic tail, is crucial for the Death-inducing Signaling Complex (DISC) formation and initiation of the apoptotic signal (Papoff et al, 1999). The third group including OPG, DcR1, DcR2, does not present any DDs. They act as decoys to compete for ligand binding and block the signaling. Nonetheless, according to some studies even other members lacking DDs can initiate apoptosis via indirect mechanisms (Oldenhuis et al, 2008). Main ligands and receptors of TNF superfamily are summarized in Table I.

PATHOPHYSIOLOGICAL ROLE OF TRAIL

While TRAIL mRNA and protein expression are found in a variety of cells and tissues (Wiley et al, 1995; Spierings et al, 2004), studies on mice and humans show that TRAIL is not expressed on the surface of freshly isolated T-cell, B-cells, monocytes, dendritic cells, natural killer (NK) cells or NKT-cells. Only a subset of mouse NK-cells expresses TRAIL at its surface. After stimulation with interferons, most NK-cells, monocytes, peripheral T-cells,

Table I. *Key members of TNF superfamily.*

Ligand	Receptor	Note
4-1BB Ligand/TNFSF9	**TNFRSF9/ 4-1BB/ILA**	It is a transmembrane cytokine and bidirectional signal transducer that acts as a ligand for **TNFRSF9**, a receptor in T lymphocytes. It's involved with his receptor in the antigen presentation process and creation of cytotoxic T cells.
APRIL/TNFSF13	**TNFRSF17/BCMA, TACI/TNFRSF13B**	It's a type II transmembrane glycoprotein important for B cell development. According to *in vitro* experiments, **APRIL**interacts with other TNF receptor family proteins like TNFRSF6/FAS and TNFRSF14/HVEM to induce apoptosis.
BAFF/BLyS/TNFSF13B/ TALL-1/THANK	**TNFRSF13B/TACI, TNFRSF17/BCMA, TNFRSF13C/BAFFR**	**BAFF,** which is expressed in B cell lineage cells, is a strong B cell activator. It'simportant in proliferation and differentiation of B cells.
CD70/CD27 Ligand/ TNFSF7	**TNFRSF27/CD27**	It is a surface antigen on activated T and B lymphocytes. It acts under many aspects: B-cell and T cell activation, cytotoxic function of natural killer cells, immunoglobulin sythesis, proliferation of costimulatedT cells, increasing the generation of cytolytic T cells.
CD30 Ligand/CD153/ TNFSF8	**TNFRSF8/CD30**	**CD30** is expressed on the surface of activated T cells, B cells and monocytes. It's a marker for Hodgkin lymphoma and inhibits the modulating Ig class switch.
CD40 Ligand/TRAP/ CD154/ TNFSF5	**CD40**	**CD40L** is mainly expressed on T cells , but also NK cells, mast cells, basophils and eosinophils. It regulates B cell function by engaging CD40 on the B cell surface.
EDA/ectodysplasin A	**EDAR,XEDAR**	**EDA** is a type II membrane protein, that acts as a homotrimer, and expressed in cells of ectodermal origin. The **EDA-A1** and **EDA-A2** splice variants differ by the deletion of two amino acids in the extracellular domain of EDA-A2. EDA-A1 binds to EDARand activates NF-kappa B signaling, whereas EDA-A2 binds to XEDAR.
Fas Ligand/FASLG/ TNFSF6/CD95L	FAS/CD95/APO-1, DcR3/ TNFRSF6B/ Decoy receptor-3	It is a transmebrane protein expressed on activated T cells and natural killer cells. It mainly induces apoptosis triggered by binding to FAS.The FAS/FASLG signaling pathway is important for immune system regulation, including activation-induced cell death (AICD) of T cells and cytotoxic T lymphocyte induced cell death. The interaction with its ligand generates death-inducing signaling complex that includes Fas-associated death domain protein (FADD), caspase 8, caspase 10. DCR3/TNFRSF6B is important for suppressing FasL- and LIGHT-mediated cell death.
GITRL/TNFSF18/ AITRL	TNFRSF18/AITR/GITR	**GITRL** modulates T lymphocyte survival in peripheral tissues and shows sequence similarily to TNF-alpha, TNF-beta, Fas Ligand and TRAIL.
LIGHT/TNFSF14/LTg/ CD258/HVEML	TNFRSF14/LIGHTR, TNFRSF3/LTβR, DcR3/TNFRSF6B	**LIGHT** plays an important role as costimulatory factor for the activation of lymphoid cells, discouraging herpesvirus infection, stimulating the proliferation of T cells, triggering apoptosis of various tumor cells, preventing tumor necrosis factor alpha mediated apoptosis in primary hepatocyte. TNFRSF14 is also known as a herpesvirus entry mediator (HVEM).
Lymphotoxin-alpha/LTA/ TNFB/TNFSF1	LTβR/TNFRSF3, TNFR1/TNFRSF1A, TNFR2/TNFRSF1B, TNFRSF14/LIGHTR	**LTA**is a cytokine produced by lymphocytes, involved in the formation of secondary lymphoid organs during development. It is highly inducible, secreted, and generates heterotrimers with lymphotoxin-beta which anchor lymphotoxin-alpha to the cell surface.Itpalys a role in inflammatory, immunostimulatory and antiviral responses and in apoptosis.

Lymphotoxin-beta/LTB/ TNFC/TNFSF3	LTBR/TNFRSF3/ LT-BETA-R	**LTB** is a type II membrane protein which anchorslymphotoxin-alpha to the cell surface through heterotrimer formation. Its main form on the lymphocyte surface is the lymphotoxin-alpha 1/beta 2 complex, which is the primary ligand for the lymphotoxin-beta receptor.
OX40 Ligand/TNFSF4/ GP34/CD252	OX40/CD134	**OX40L** is expressed on the surface of activated B cells, T cells, dendritic cells and endothelial cells; interactions and mediates adhesion of activated T cells to endothelial cells. Interacting with adaptor proteins TRAF2 and TRAF5 OXO40 activates NF-kappaB, and suppresses apoptosis.
TL1A/TNFSF15/VEGI	TNFRSF25/DR3, TNFRSF6B/DcR3	**TL1A** is a protein largely expressed by endothelial cells.Its expression is inducible by TNF-alpha and IL-1alpha. It inhibits endothelial cell proliferation and acts as an angiogenesis inhibitor. It can activate NF-kappaB and MAP kinases.
TNF-alpha/TNFA/ TNFSF2	TNFRSF1A/TNFR1, TNFRSF1B/TNFBR/ TNFR2	It is a cytokine mainly secreted by macrophages, and plays a role in cell proliferation, differentiation, apoptosis, lipid metabolism, and coagulation.
TRAIL /CD253/ Apo-2L/TNFSF10	TNFRSF10A/TRAILR1/ DR4, TNFRSF10B/ TRAILR2/ DR5, TNFRSF10C/ TRAILR3/ DcR1, TNFRSF10D/ TRAILR4/ DcR2, TNFRSF11B/OPG	**TRAIL** is the most homologous TNF superfamily members to Fas Ligand. Infact 28% of amino acid sequence identity in its extracellular domain is the same as the Fas Ligand. The binds with its receptors trigger the activation of MAPK8/JNK, caspase 8, and caspase3.
TRANCE/OPGL/ RANKL/TNFSF11	TNFRSF11B/OPG, RANK/TNFRSF11A	**OPGL** is an adentritic cell survival factor mainly expressed in T cells and T cell rich organs, like thymus and lymph nodes. It regulates T cell-dependent immune response and may regulate cell apoptosis, Infact it activates antiapoptotic kinase AKT/PKB through a signaling complex involving SRC kinase and tumor necrosis factor receptor-associated factor (TRAF) 6.
TWEAK/APO3L/ TNFSF12	FN14/TWEAKR	It is a cytokine existing in membrane-bound and secreted forms. It can induce apoptosis, promote proliferation and migration of endothelial cells, and regulates angiogenesis.

and dendritic cells express TRAIL, suggesting an important role of TRAIL in innate immune responses (Smyth et al, 2003). Furthermore, TRAIL contributes to host immunosurveillance against primary tumour development; in fact, neutralization of TRAIL promoted tumour development in mice inoculated with the carcinogen methylcholanthrene (MCA) (Takeda et al, 2002). In the same line, such increased tumour promoting effect of MCA was also observed in TRAIL$^{-/-}$ mice (Cretney et al, 2002). Moreover, the preferential emergence of TRAIL-sensitive fibrosarcoma cells in TRAIL$^{-/-}$ mice and IFNγ-deficient mice implies an immune selection pressure against TRAIL-sensitive cells during tumour development (Takeda et al, 2002). In addition to such TRAIL's proposed role in tumour immune surveillance, various roles have been proposed for TRAIL in autoimmunity. Most studies report an inhibitory function of TRAIL on the development of experimentally-induced autoimmune diseases in mouse models, such as rheumatoid arthritis, diabetes and experimental autoimmune encephalomyelitis. However, TRAIL may also be involved in rapid progression of autoimmune diseases (Cretney et al, 2006). Thus, TRAIL may exert dual functions depending on time, extent and location of its expression. Besides studies performed on mice, other studies report increased serum levels of soluble TRAIL (sTRAIL) in patients with neoplastic, autoimmune and infectious diseases. In a human endotoxemia model, sTRAIL levels increased 10-fold after the administration of endotoxin (Lub-de Hooge et al, 2004). Patients with systemic lupus erythematosus display raised sTRAIL concentrations (Lub-de Hooge et al, 2005), and in human multiple sclerosis patients sTRAIL levels might serve as a potential response marker for IFN-β treatment (Cretney et al, 2006). In addition, TRAIL has been shown to activate inflammation, proliferation, migration, and invasion in cancer cells (Secchiero et al, 2003). Induction of inflammation by TRAIL occurs through activation of NF-kB and subsequent

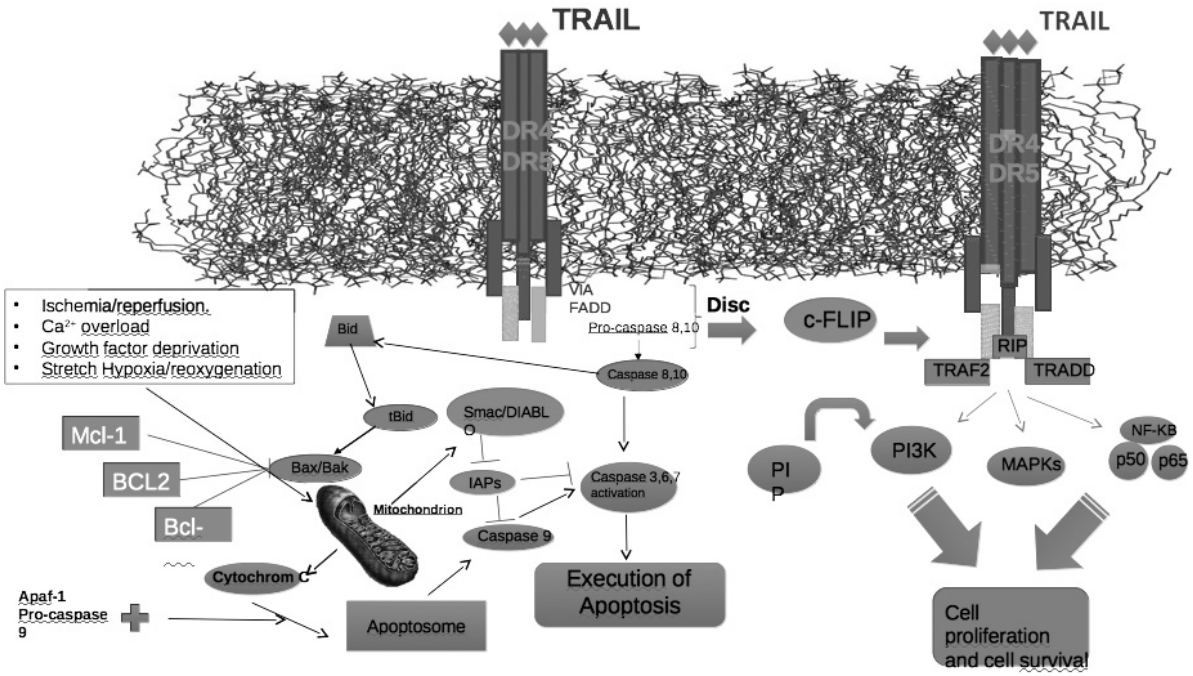

Fig. 1. *Schematic representation of the TRAIL death pathway.*

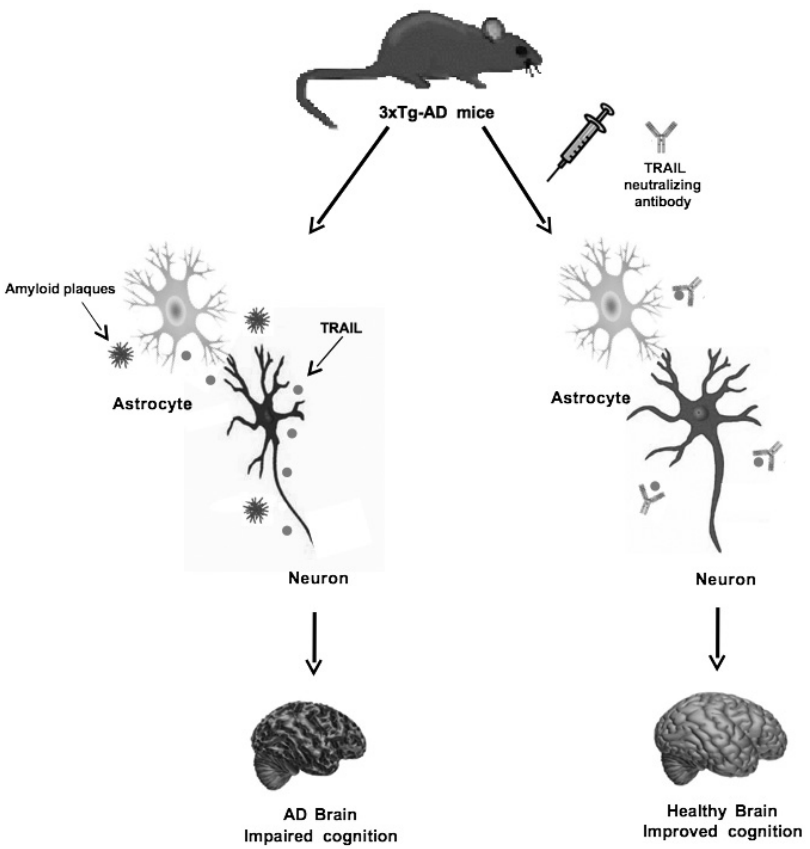

Fig. 2. *Immunoneutralization of TRAIL ameliorates functional outcome in the 3xTg-AD mice.*

production of cytokines (Choi et al, 2002). *In vivo* studies showed that TRAIL$^{-/-}$ mice were protected from ovalbumin-induced development of airway hyper-reactivity and peribronchial eosinophilia, and had reduced levels of mast cells in their airways, correlated with lower levels of T helper type 2 (Th2) cytokines including interleukin (IL)-4, -5, -10, and -13 and chemokines (Collison et al, 2014).

By contrast, other studies showed that TRAIL-deficient mice exhibited an enhanced inflammatory response with increased neutrophil numbers and reduced neutrophil apoptosis (McGrath et al, 2011). TRAIL treatment also reduced the severity and incidence of inflammatory disorders such as joint swelling, erythema, and edema, by inhibiting inflammatory cell infiltration, cartilage destruction, and bone erosion in the joints of TRAIL-treated mice. Because of its anti-inflammatory activities, TRAIL appears involved in inhibition of allergic airway disease (Faustino et al, 2014), attenuation of metabolic abnormalities (Bernardi et al, 2012), suppression of diabetic neuropathy, and inverse association with mortality risk in chronic kidney disease patients (Malyszko et al, 2011). These data, however, are in contrast with reports that TRAIL can directly activate NF-kB (DegliEsposti et al, 1997). TRAIL expression has also been shown to positively correlate with osteolytic markers, such as serum calcium and urinary deoxypyridinoline in multiple myeloma patients, suggesting that TRAIL plays a role in bone resorption (Kawano et al, 2012). *In vitro* studies showed that TRAIL also induces osteoclast differentiation mediated through the TNF receptor-associated factor 6 (TRAF-6)-dependent signaling pathway (Yen et al, 2012). In addition, in peripheral blood mononuclear cells (PBMCs) from healthy donors, TRAIL directly induced osteoclast formation in the absence of receptor activator of NF-kB ligand (RANKL), whereas it exerted an inhibitory effect when added concomitantly with RANKL (Brunetti et al, 2011).

It has been demonstrated that binding of TRAIL to DR4, DR5, or even DcR2, induces NF-kB activation through the regulation of RIP, which activates survival signaling in tumor cells (Ehrhardt et al, 2003). In the absence of caspase-8, TRAIL has been shown to induce proliferative and survival signals in small-cell lung cancer cells through DR5 expression and phosphorylation of ERK1/2 (Belyanskaya et al, 2008). TRAIL also increases the proliferation of TRAIL-resistant glioma cells by increased phosphorylation of ERK1/2 (Vilimanovich et al, 2008).

TRAIL-induced migration and invasivity is reported in various types of cancer cells. In TRAIL-resistant cholangiocarcinoma cells, TRAIL has been shown to promote NF-kB-dependent tumor cell migration and invasion, but not proliferation (Ishimura et al, 2006). By contrast, another study showed that TRAIL suppresses chemokine receptor CXCR4-mediated human breast cancer MDA-MB-231 cell migration by upregulating miR-146a expression through NF-kB (Wang et al, 2013). Low doses of TRAIL induced the migration of human mesenchymal stem cells, depending upon the phosphorylation of ERK1/2 (Secchiero et al, 2008). TRAIL also stimulated protein kinase B (PKB)/Akt, and induced migration and vessel tube formation in human umbilical vein endothelial cells (HUVECs) (Secchiero et al, 2004). In a human pancreatic adenocarcinoma xenograft animal model, TRAIL promoted the development of liver metastases (Trauzold et al, 2006).

Furthermore, the non-apoptotic function of TRAIL is demonstrated by its effect on the expression of inflammatory molecules. TRAIL has been shown to induce urokinase plasminogen activator (uPA) and IL-8 expression in pancreatic ductal adenocarcinoma (PDAC) cells (Zhou et al, 2013).

TRAIL also induced monocyte migration mediated by DR4 via the Rho GTPasesignaling pathway (Wei et al, 2010).

TRAIL IN CENTRAL NERVOUS SYSTEM DISORDERS

All TRAIL death and decoy receptors are expressed in the healthy human brain (Dörr et al, 2002; Cannella et al, 2007). In normal human brain samples, TRAIL mRNA or protein was not detected in one study (Dörr et al, 2002), while other Authors found barely detectable TRAIL immunoreactivity, which was restricted to oligodendrocytes (Cannella et al, 2007). Brain macrophages have been shown to upregulate TRAIL upon activation (e.g., in brain samples from patients with HIV-associated encephalitis) (Ryan

et al, 2004). TRAIL receptors are also found on neurons, astrocytes and oligodendrocytes (Dörr et al, 2002; Cannella et al, 2007). Differences between the mentioned studies may in part relate to the origin of the tissue samples, i.e., freshly obtained surgical specimens (Dörr et al, 2002) compared to brain bank tissue with a 6- to 9-h post-mortem interval (Cannella et al, 2007). Despite these ambiguities, it appears that the normal brain expresses very low levels of TRAIL; healthy oligodendrocytes and neurons seem to express few TRAIL death receptors in contrast to a relative abundance of TRAIL decoy receptors. Such low level of TRAIL conflicts with earlier speculations that constitutive expression of TRAIL at the blood–brain barrier may add to the brain's special immunology by presenting apoptotic signals to antigen-specific T cells, as had been previously demonstrated for the TNF and CD95 systems in the brain (Bechmannet al, 1999*;* Flugelet al, 2000; Pratet al, 2001; Bechmann et al, 2002). The presence of TRAIL death receptors on brain parenchymal cells suggests a potential role for TRAIL as a mediator of neuronal and glial apoptosis (Dörr et al, 2002). Indeed, primary human neurons (Ryan et al, 2004) as well as neurons, oligodendrocytes, astrocytes and microglial cells in human brain explant cultures (Nitsch et al, 2000) undergo apoptosis upon stimulation with recombinant human TRAIL.

Under pathological conditions, such as multiple sclerosis (Cannella et al, 2007), experimental autoimmune encephalitis (EAE) in mice (Aktas et al, 2003), or Alzheimer's disease (Uberti et al, 2004), TRAIL and its death and decoy receptors are differentially regulated. TRAIL and TRAIL receptor RNA were also detected in brain tumour samples from patients (Frank et al, 1999). In cell culture, proinflammatory stimuli such as IFN-γ or LPS induce TRAIL expression in murine microglia and foetal astrocytes (Lee et al, 2003; Genc et al, 2003).

TRAIL signalling seems not exclusively linked to apoptosis induction in target cells, but may, in turn, also trigger pro-inflammatory and pro-survival pathways. For example, human astrocytes have been shown to upregulate ICAM-1 in response to TRAIL (Choi et al, 2008), and cultured brain microvascular endothelial cells displayed activation of MMP9 by TRAIL via DR5, although to a lesser extent than in response to signalling via CD95 (Wosik et al, 2007).

a. TRAIL in Alzheimer's disease

Specifically, TRAIL has been shown to play a pivotal role in neuroinflammatory processes associated with different causes of neurodegeneration. The effects of TRAIL on degenerating neurons were first discovered in 2003, when Cantarella et al, demonstrated that the challenge of differentiated human neuroblastoma cells with amyloid beta induced increased amounts of TRAIL and its DR4 and DR5 death receptors. In further experiments, showing that TRAIL sets into motion the apoptotic machine via activation of the extrinsic caspase pathway, knocking down the adapter protein FADD resulted in protection of cells from amyloid-induced damage and death and, in addition, a similar effect was obtained using inhibitors of caspases. In these preliminary experiments, Authors also demonstrated that neutralization of TRAIL by means of a specific, anti-TRAIL, monoclonal antibody, rescued at least seventy to eighty percent of differentiated neuroblastoma cells challenged with amyloid from death *in vitro.*

The idea that TRAIL is a potent mediator of cell death and underlying neuroinflammation was first confirmed by other data from histology of post-mortem human AD brain. In fact, when immunohistochemistry for TRAIL was performed in specimens stained with the red congo method to detect amyloid, interestingly, immunostained neurons and glia were localized in the vicinity of amyloid plaques (Uberti et al, 2004).

Indeed, the effect of TRAIL *in vitro* appears quite potent, and, thus, one could speculate that such an effect could be contributed by contemporary activation of multiple signalling pathways. Indeed, alterations of the Wnt pathway are present in different conditions reproducing Alzheimer'sdisease, and such dysfunctions are likely to promote hyperphosphorylation of the tau protein with consequent downstream formation of intracellular neurofibrillary tangles, together with plaques, another pathological landmark of the AD brain. Cantarella et al, (2008) observed that TRAIL influenced the function of the Wnt receptor in the same cells, leading to consequent phosphorylation of beta-catenin and hyperphosphorylation of the tau protein, eventually paralleled by activation of caspases and neuronal cell death *in vitro*.

Thus, simultaneous activation of the caspases and hyperphsphorylation of the tau protein could well explain the potent action of TRAIL as a mediator of amyloid neurotoxicity (Cantarella et al, 2008). Together with data showing that TRAIL is released by activated glia during neuroinflammatory processes along with other inflammatory mediators, such as, for example, nitric oxide, there is a body of evidence that the cytokine could play a role in a complex system *in vitro* (Cantarella et al, 2007). The confirmation of this hypothesis comes from data showing the beneficial effects of an anti-TRAIL treatment in a strain of mice which spontaneously underwent age-related cognitive decline, the murine triple transgenic model of Alzheimer's disease 3xTg-AD. This species bears a triple mutation and displays cognitive deficits increasing proportionally to their age. The Morris Water Maze (MWM) test is commonly used to check the cognitive status of rats and mice with the aim of evaluating the influence of an array of factors upon cognitive function and memory. Discrete brain areas of the 3xTg-AD mice, with special regard to the hippocampus, express amyloid, which increases proportionally to age. Also the expression of TRAIL and its death receptors, as well as that of inflammatory mediators and gliosis, is increased in the 3xTg-AD mice hippocampus and correlates well with the cognitive deficit affecting the animals. Treatment of three-month-old 3xTg-AD mice with a TRAIL neutralizing monoclonal antibody results in dramatic improvement of cognitive decline, assessed by the MWM test, which is paralleled by significant decrease of expression of TRAIL itself and its death receptor in the hippocampus. The treatment consists of the intraperitoneal injection of the an anti-TRAIL monoclonal antibody. The latter crosses the blood brain barrier of 3xTg-AD mice and is localized in the brain, and, more specifically in the hippocampus, as demonstrated by immunofluorescence experiments. Such functional recovery is paralleled by significantly attenuated expression of inflammatory mediators in the brain, as well as by recovery of gliosis, which is richly represented in untreated animals (Cantarella et al, 2015) (Fig. 2).

b. TRAIL in neurotrauma

Increased expression of inflammatory molecules and gliosis are also features of the nervous tissue which had been subjected to a traumatic event (Kamphuis et al, 2014). For example, in a mouse model of spinal cord injury (SCI), the expression of mediators of the inflammatory/immune response is significantly increased (Nocentini et al, 2008), and it is amplified proportionally timewise after trauma (Cuzzocrea et al, 2006). On the basis of both the role of TRAIL in amyloid-related neurodegeneration, as well as of the prominent neuroinflammation affecting traumatized tissues, Cantarella et al, (2010) have shown that the expression of TRAIL and its death receptors DR4 and DR5 are significantly increased in the peritraumatic area in the spinal cord of mice which had undergone the SCI procedure. Trauma is associated with a severe deficit of motor activity, mainly localized in the posterior forelimbs; such motor deficit worsens progressively until it stabilizes to a given grade of severity (Schrimsher and Reier, 1992). The expression of iNOS, IL-1 beta and COX2 in the spinal cord of these animals parallels with the functional deficit, along with increased population of glial cells around the lesion. In such model of SCI, when the animals are pretreated with a TRAIL-neutralizing antibody, the enlargement of the SCI is significantly slower and relatively limited, resulting in diminished neuroinflammation and expression of inflammatory mediators, as well as by substantial functional recovery (Cantarella et al, 2010).

c. TRAIL in brain ischemia

Stroke is a major cause of cardiovascular death in the adults of western countries, resulting in disability (Donna et al, 2008). Brain ischemia which underlies stroke is associated with progressive enlargement of the damaged areas and prominent inflammation, with subsequent irreversible neuronal damage (Muir et al, 2007). Now, evidence shows that the resistance of the nervous tissue to ischemia is increased by previous exposure to non-injurious pre-conditioning (PC) stimulus (Gidday, 2006). In fact, PC acts by preventing the spreading of the penumbra area and the recruitment of neurons to apoptotic death (Nakajima et al, 2004). PC is detected by sensor mediators of the inflammatory response, such as cytokines, which are the orchestra of detrimental factors fuelling the progressive post-ischemic damage in the nervous tissue. Among cytokines, TRAIL is endowed with potent neurotoxic effects,

and is produced by either peripheral immunocytes (Falschlehner et al, 2009) or by CNS resident cells, such as neurons and microglia (Cantarella et al, 2003; Cantarella et al, 2004). Interestingly, whereas 100-min transient ischemia, followed by 24 h reperfusion, results in substantial post-ischemic damage in the rat, the same harmful ischemia preceded by a 30-min ischemia does not reach the grade of severity in terms of tissue parameter impairment and functional outcome. It now appears that TRAIL plays a pivotal role in the post-ischemic inflammatory processes, as pretreatment with a TRAIL-neutralizing antibody does imply less severe damage in the ischemic tissues. Moreover, prolonged ischemia induces the expression of TRAIL and both its death receptors, DR4 and DR5, whereas it dramatically decreases that of decoy, TRAIL neutralizing receptors DcR1 and DcR2. Contrarywise, the latter is significantly augmented by PC, suggesting that, probably, self-neutralization of TRAIL is one of the mechanisms contributing to the neuroprotective effects of PC (Cantarella et al, 2014).

It has been demonstrated that cytokines may exert modulatory effects on mood and cognition, through their modulation of neuronal function. The link between the effect of pro-inflammatory cytokines and the development of cognitive and emotional disorders has been associated to different effects. It has been shown that the chronic impact of pro-inflammatory cytokines may impair neuroplasticity, therefore contributing to the development of cognitive and mood disorders (McAfoose and Baune, 2009). Among these, increased levels of TNF-α have been associated with impaired neuroplasticity and to inhibit long-term potentiation (LTP) (Butler et al, 2004). The role of cytokines, and their unbalance, in the origin and development of cognitive and mood disorders has been extensively studied and demonstrated, although the underlying mechanisms are still elusive (Maes et al, 2009, Dantzer et al, 2009). Among the current hypotheses, it has been shown that chronic stress may lead to unbalance of different cytokines, which in turn has been associated with alteration in other systems, including HPA axis hyperactivity (Maes et al, 1993) and altered serotonergic and dopaminergic activity. (Bonaccorso et al, 2002), which are typically associated with anxiety and mood disorders. In this regard, pro-inflammatory cytokines may stimulate the release of CRF, therefore activating the HPA axis (Besedovsky et al, 1991, Pace et al, 2007), with the resulting hypercortisolism, commonly observed in chronic stress and mood disorders. Pro-inflammatory cytokines have also been associated with enhanced re-uptake of neurotransmitters, therefore decreasing their concentrations in the synaptic cleft. It has been shown that cytokines such as IL-1 and TNF may stimulate the uptake of serotonin (Zhu et al, 2006), which is also associated with symptoms of depression. Moreover, it has been observed that major depression may induce increased inflammatory responses to stress, and this has been observed mostly in patients exposed to early life stress, therefore suggesting a link between early life stress and increased inflammatory responses to stress later in life (Haroon et al, 2012). Therefore, these observations supporting the immunologic/inflammatory hypothesis of depression (Leonard, 2010), together with the fact that TRAIL plays a critical role in neuro-inflammatory processes associated with different causes of neurodegeneration, and the possibility that these neurodegenerative processes may affect critical structures involved in the regulation of cognitive and emotional processes, such as the hippocampus and prefrontal cortex, suggests the potential role of TRIAL in the origin and development of cognitive and emotional disorders.

POTENTIAL ROLE OF TRAIL IN MOOD DISORDERS

It has been demonstrated that cytokines may exert modulatory effects on mood and cognition, through their modulation of neuronal function. The link between the effect of pro-inflammatory cytokines and the development of cognitive and emotional disorders has been associated to different effects. It has been shown that the chronic impact of pro-inflamatory cytokines may impair neuroplasticity, therefore contributing to the development of cognitive and mood disorders (McAfoose and Baune, 2009). Among these, increased levels of TNF-α have been associated with impaired neuroplasticity and to inhibit long-term potentiation (LTP) (Butler et al, 2004). The role of

cytokines, and their disbalance, in the origin and development of cognitive and mood disorders has been extensively studied and demonstrated, although the underlying mechanisms are still elusive (Maes et al, 2009, Dantzer et al, 2009). Among the current hypotheses, it has been shown that chronic stress may lead to disbalance of different cytokines, which in turn has been associated with alteration in other systems, including HPA axis hyperactivity (Maes et al, 1993) and altered serotonergic and dopaminergic activity (Bonaccorso et al, 2002), which are typically associated with anxiety and mood disorders. In this regard, pro-inflamatory cytokines may stimulate the release of CRF, therefore activating the HPA axis (Besedovsky et al, 1991, Pace et al, 2007), with the resulting hypercortisolism, commonly observed in chronic stress and mood disorders. Pro-inflammatory cytokines have also been associated with enhanced re-uptake of neurotransmitters, therefore decreasing their concentrations in the synaptic cleft. It has been shown that cytokines such as IL-1 and TNF may stimulate the uptake of serotonin (Zhu et al, 2006), which is also associated with symptoms of depression. Moreover, it has been observed that major depression may induce increased inflammatory responses to stress, and this has been observed mostly in patients exposed to early life stress, therefore suggesting a link between early life stress and increased inflammatory responses to stress later in life (Haroon et al, 2012). Therefore, these observations supporting the immunologic/inflammatory hypothesis of depression (Leonard, 2010), together with the fact that TRAIL plays a critical role in neuroinflammatory processes associated with different causes of neurodegeneration, and the possibility that these neurodegenerative processes may affect critical structures involved in the regulation of cognitive and emotional processes, such as the hippocampus and prefrontal cortex, suggest the potential role of TRIAL in the origin and development of cognitive and emotional disorders.

THE TRAIL PATHWAY: IS NEUROINFLAMMATION A COMMON CLUE FOR THERAPEUTIC INTERVENTION IN CNS DISORDERS?

TRAIL is abundantly expressed along with its death receptors DR4 and DR5 in neurodegenerative processes, regardless of their respective causes, either amyloid, trauma, or ischemia. All these conditions, nevertheless, are characterized by the presence of prominent neuroinflammation, and TRAIL seems to exert particularly prominent detrimental effects. The potency of TRAIL effects could be justified by two reasons: 1. All noxious causes would robustly increase the expression of functional DR4 and DR5 receptors in the injuried brain tissue; 2. TRAIL itself definitely appears as a potent inducer of the expression of inflammatory molecules and, in a way, it conducts the orchestra of inflammatory factors. Interactions among cytokines are characterized by either additive effects and redundancy, probably to perpetuate and enlarge the detrimental effects triggered independently by each one of them; 3. Noxious stimuli activate glia and, consequently, its cytokine/inflammatory products, including eicosanoids and cytokines. In definite situations, such a cytokine scenario would also imply activation of protective mechanisms against the detrimental effects of TRAIL, such as increased expression of the decoy receptor proteins, caused by protective strategies, including TRAIL pharmacological neutralization or ischemic preconditioning.

CONCLUSIONS

In the light of the bulk of literature data, it is plausible to hypothesize that targeting the TRAIL machinery set into motion by neurodegenerative causes, could be an effective action to restrain neuronal death and consequent functional deficit associated with neurodegenerative processes. Indeed, an innovative therapeutic approach to neurodegenerative disorders could be envisioned by proper immunopharmacological manipulation of the neuroinflammatory orchestra.

REFERENCES

Aktas O, Waiczies S, Smorodchenko A, Dorr J et al. and Zipp F (2003) Treatment of relapsing paralysis in experimental encephalomyelitis by targeting Th1 cells through atorvastatin. *J Exp Med* **197**: 725-733.

Almasan A, Ashkenazi A (2003) Apo2L/TRAIL: apoptosis signaling, biology, and potential for cancer

therapy. *Cytokine Growth Factor Rev* **14**: 337-348.

Aukrust P, Sandberg WJ, Otterdal K, Vinge LE et al. and Ueland T (2001) Tumor necrosis factor superfamily molecules in acute coronary syndromes. *Ann Med* **43**: 90-103.

Bechmann I, Mor G, Nilsen J, Eliza M, Nitsch R, Naftolin F (1999) FasL (CD95L, Apo1L) is expressed in the normal rat and human brain: evidence for the existence of an immunological brain barrier. *Glia* **27**: 62-74.

Bechmann I, Steiner B, Gimsa U, Mor G et al. and Zipp F (2002) Astrocyte-induced T cell elimination is CD95 ligand dependent. *J Neuroimmunol* **132**: 60-65.

Belyanskaya LL, Ziogas A, Hopkins-Donaldson S, Kurtz S, Simon HU, Stahel R, Zangemeister-Wittke U (2008) TRAIL-induced survival and proliferation of SCLC cells is mediated by ERK and dependent on TRAIL-R2/DR5 expression in the absence of caspase-8. *Lung Cance r***60**: 355-365.

Bernardi S, Zauli G, Tikellis C, Candido R et al. And Thomas MC (2012) TNF-related apoptosis-inducing ligand significantly attenuates metabolic abnormalities in high-fat-fed mice reducing adiposity and systemic inflammation. *Clin Sci (Lond)* **123**: 547-555.

Besedovsky HO, del Rey A, Klusman I, Furukawa H, MongeArditi G, Kabiersch A (1991) Cytokines as modulators of the HPA axis *J Steroid Biochem Mol Biol* **40**:613-618.

Bhardwaj A, Aggarwal BB (2003) Receptor-mediated choreography of life and death. *J Clin Immunol* **23**: 317-332.

Bodmer JL, Meier P, Tschopp J, Schneider P (2000) Cysteine 230 is essential for the structure and activity of the cytotoxic ligand TRAIL. *J Biol Chem* **275**: 20632-20637.

Bodmer JL, Schneider P, Tschopp J (2002) The molecular architecture of the TNF superfamily. *Trends Biochem Sci* **27**: 19-26.

Bonaccorso S, Marino V, Puzella A, Pasquini M et al. and Maes M (2002) Increased depressive ratings in patients with hepatitis C receiving interferonalpha-based immunotherapy are related to interferon-alpha-induced changes in the serotonergic system. *J Clin Psychopharmacol* **22**:86-90.

Bouralexis S, Findlay DM, Evdokiou A (2005) Death to the bad guys: targeting cancer via Apo2L/TRAIL. *Apoptosis* **10**: 35-51.

Brunetti G, Oranger A, Mori G, Sardone F et al. and Colucci S (2011) TRAIL effect on osteoclast formation in physiological and pathological conditions. *Front Biosci (Elite Ed)* **3**: 1154-1161.

Butler MP, O'Connor JJ, Moynagh PN (2004) Dissection of tumor-necrosis factor-alpha inhibition of longterm potentiation (LTP) reveals a p38 mitogen-activated protein kinase-dependent mechanism which maps to early-but not late-phase LTP. *Neuroscience* **124**:319-326.

Cannella B, Gaupp S, Omari KM, Raine CS (2007) Multiple sclerosis: death receptor expression and oligodendrocyte apoptosis in established lesions. *J Neuroimmunol* **188**: 128-137.

Cantarella G, Uberti D, Carsana T, Lombardo G, Bernardini R, Memo M (2003) Neutralization of TRAIL death pathway protects human neuronal cell line from beta-amyloid toxicity. *Cell Death Differ* **10**: 134-41.

Cantarella G, Risuglia N, Lombardo G, Lempereur L et al. and Bernardini R (2004) Protective effects of estradiol on TRAIL-induced apoptosis in a human oligodendrocytic cell line: evidence for multiple sites of interactions. *Cell Death Differ* **11**: 503-511.

Cantarella G, Lempereur L, D'Alcamo MA, Risuglia N et al. and Bernardini R (2007) Trail interacts redundantly with nitric oxide in rat astrocytes: potential contribution to neurodegenerative processes. *J Neuroimmunol* **182**: 41-47.

Cantarella G, Di Benedetto G, Pezzino S, Risuglia N, Bernardini R (2008) TRAIL-related neurotoxicity implies interaction with the Wnt pathway in human neuronal cells in vitro. *J Neurochem* **105**: 1915-1923.

Cantarella G, Di Benedetto G, Scollo M, Paterniti I et al. and Bernardini R (2010) Neutralization of tumor necrosis factor-related apoptosis-inducing ligand reduces spinal cord injury damage in mice. *Neuropsychopharmacology* **35**: 1302-1314.

Cantarella G, Pignataro G, Di Benedetto G, Anzilotti S et al. and Bernardini R (2014) Ischemic tolerance modulates TRAIL expression and its receptors and generates a neuroprotected phenotype. *Cell Death Dis***17**: e1331. doi: 10.1038/cddis.2014.286

Cantarella G, Di Benedetto G, Puzzo D, Privitera L et al. and Bernardini R (2015) Neutralization of TNFSF10 ameliorates functional outcome in a murine model of Alzheimer's disease. *Brain* **138**: 203-216.

Capuron L, Miller AH (2011) Immune system to brain signaling: neuropsychopharmacological implications. *Pharmacol Ther* **130**:226-238.

Choi K, Song S, Choi C (2008) Requirement of caspases and p38 MAPK for TRAIL-mediated ICAM-1 expression by human astroglial cells. *Immunol Lett* **117**: 168-173.

Collison A, Li J, Pereira de Siqueira A, Zhang J et al. and Mattes J (2014) TRAIL regulates hallmark features of airways remodelling in allergic airways disease. *Am J Respir Cell MolBiol* **51**: 86-93.

Cretney E, Takeda K, Yagita H, Glaccum M, Peschon JJ, Smyth MJ (2002) Increased susceptibility to tumor initiation and metastasis in TNF-related apoptosis-inducing ligand-deficient mice. *J Immunol* **168**: 1356-1361.

Cuzzocrea S, Genovese T, Mazzon E, Crisafulli C, et al. and Thiemermann C (2006) Glycogen synthase kinase-3 beta inhibition reduces secondary damage in experimental spinal cord trauma. *J Pharmacol Exp Ther* **318**: 79-89.

Dantzer R (2009) Cytokines, sickness behavior, and depression *Immunol Allergy Clin North Am* **29**:247-264.

Darnay BG, Ni J, Moore PA, Aggarwal BB (1999) Activation of NF-kappaB by RANK requires tumor necrosis factor receptor-associated factor (TRAF) 6 and NF-kappaB-inducing kinase. Identification of a novel TRAF6 interaction motif. *J Biol Chem* **274**: 7724-31.

Degli-Esposti MA, Dougall WC, Smolak PJ, Waugh JY, Smith CA, Goodwin RG (1997) The novel receptor TRAIL-R4 induces NF-kappaB and protects against TRAIL-mediated apoptosis, yet retains an incomplete death domain. *Immunity***7**: 813-820.

Donnan GA, Fisher M, Macleod M, Davis SM (2008) Stroke. *Lancet* **371**: 1612-1623.

Dörr J, Bechmann I, Waiczies S, Aktas O et al. and Zipp F (2002) Lack of tumor necrosis factor-related apoptosis-inducing ligand but presence of its receptors in the human brain. *J Neurosci* **22**: RC209.

Duiker EW, Mom CH, de Jong S, Willemse PHB, Gietema JA, van der Zee AGJ, de Vries EGE (2006) The clinical trail of TRAIL. *Eur J Canc* **42**: 2233-2240.

Ehrhardt H, Fulda S, Schmid I, Hiscott J, Debatin KM, Jeremias I (2003) TRAIL induced survival and proliferation in cancer cells resistant towards TRAIL-induced apoptosis mediated by NF-kappaB. *Oncogene* **22**: 3842-3852.

Falschlehner C, Schaefer UandWalczak H (2009) Following TRAIL's path in the immune system. *Immunology* **127**: 145-54.

Faustino L, Fonseca DM, Florsheim EB, Resende RR et al. and Russo M (2014) Tumor necrosis factor-related apoptosis-inducing ligand mediates the resolution of allergic airway inflammation induced by chronic allergen inhalation. *Mucosal Immunol* **7**: 1199-1208.

Flugel A, Schwaiger FW, Neumann H, Medana I et al. and Graeber MB (2000) Neuronal FasLinduces cell death of encephalitogenic T lymphocytes. *Brain Pathol* **10**: 353-364.

Frank S, Köhler U, Schackert G, Schackert HK (1999) Expression of TRAIL and its receptors in human brain tumors. *Biochem Biophys Res Commun***2 57**: 454-459.

Fulda S, Debatin KM (2004) Modulation of TRAIL signaling for cancer therapy. *Vitam Horm* **67**: 275-90.

Gaur U, Aggarwal BB (2003) Regulation of proliferation, survival and apoptosis by members of the TNF superfamily. *Biochem Pharmacol* **66**: 1403-1408.

Genc S, Kizildag S, Genc K, Ates H, Atabey N (2003) Interferon gamma and lipopolysaccharide upregulate TNF-related apoptosis-inducing ligand expression in murine microglia. *Immunol Lett* **85**: 271-274.

Gidday JM (2006) Cerebral preconditioning and ischaemic tolerance. *Nat Rev Neurosci* **7**: 437-448.

Guo Y, Chen C, Zheng Y, Zhang Jet al. and Liu Y (2005) A novel anti-human DR5 monoclonal antibody with tumoricidal activity induces caspase-dependent and caspase-independent cell death. *J Biol Chem* **280**: 41940-41952.

Haroon E, Raison CL, Miller AH (2102) Psychoneuroimmunology Meets Neuropsychopharmacology: Translational Implications of the Impact of Inflammation on Behavior. *Neuropsychopharmacology Rev* **37**:137-162.

Held J, Schulze-Osthoff K (2001) Potential and caveats of TRAIL in cancer therapy. *Drug Resist Updat* **4**: 243-52.

Huang Y, Erdmann N, Peng H, Zhao Y, Zheng J (2005) The role of TNF Related Apoptosis-Inducing Ligand in neurodegenerative diseases. *Cell Mol Immunol* **2**: 113-122.

Hymowitz SG, O'Connel MP, Ultsch MH, Hurst

A et al. and Kelley RF (2000) A unique zinc-binding site revealed by a highresolution X-ray structure of homotrimeric Apo2L/TRAIL. *Biochemistry* **39**: 633-640.

Ishimura N, Isomoto H, Bronk SF, Gores GJ (2006) Trail induces cell migration and invasion in apoptosis-resistant cholangiocarcinoma cells. *Am J Physiol Gastrointest Liver Physiol* **290**: G129-G136.

Jo M, Kim TH, Seol DW, Esplen JE, Dorko K, Billiar TR, Strom SC (2000) Apoptosis induced in normal human hepatocytes by tumor necrosis factor-related apoptosis-inducing ligand. *Nature Med* **6**: 564-567.

Kamphuis W, Middeldorp J, Kooijman L, Sluijs JA, et al. and Hol EM (2014) Glial fibrillary acidic protein isoform expression in plaque related astrogliosis in Alzheimer's disease. *Neurobiol Aging* **35**: 492-510.

Kawano Y, Ueno S, Abe M, Kikukawa Y et al. and Hata H (2012) TRAIL produced from multiple myeloma cells is associated with osteolytic markers. *Oncol Rep* **27**: 39-44.

LeBlancHN, Ashkenazi A (2003) Apo2L/TRAIL and its death and decoy receptors. *Cell Death Diff* **10**: 66-75.

Lee J, Shin JS, Park JY, Kwon D, Choi SJ, Kim SJ, Choi IH (2003) p38 mitogen-activated protein kinase modulates expression of tumor necrosis factor-related apoptosis-inducing ligand induced by interferon-gamma in fetal brain astrocytes. *J Neurosci Res* **74**: 884-890.

Leonard BE (2010) The concept of depression as a dysfunction of the immune system. *Curr Immunol Rev* **6**: 205-212.

Lub-de Hooge MN, de Jong S, Vermot-Desroches C, Tulleken JE, de Vries EG, Zijlstra JG (2004) Endotoxin increases plasma soluble tumor necrosis factor-related apoptosis-inducing ligand level mediated by the p38 mitogen-activated protein kinase signaling pathway. *Shock* **22**: 186-8.

Lub-de Hooge MN, de Vries EG, de Jong S, Bijl M (2005) Soluble TRAIL concentrations are raised in patients with systemic lupus erythematosus. *Ann Rheum Dis* **64**: 854-8.

Maes M, Scharpe S, Meltzer HY, Bosmans E, Suy E, Calabrese J, Cosyns P (1993) Relationships between interleukin-6 activity, acute phase proteins, and function of the hypothalamic–pituitary–adrenal axis in severe depression. *Psychiatry Res* **49**:11-27.

Maes M,Yirmyia R, Noraberg J, Brene Set al. andMaj M (2009) The inflammatory & neurodegenerative (I&ND) hypothesis of depression: leads for future research and new drug developments in depression. *Metab Brain Dis* **24**:27-53.

Malyszko J, Przybylowski P, Malyszko J, Koc-Zorawska E, Mysliwiec M (2011) Tumor necrosis factor-related apoptosis- inducing ligand is a marker of kidney function and inflammation in heart and kidney transplant recipients. *Transplant Proc* **43**: 1877-1880.

Martin-Villalba A, Herr I, Jeremias I, Hahne M et al. and Debatin KM (1999) CD95 ligand (Fas-L/APO-1L) and tumor necrosis factor-related apoptosis-inducing ligand mediate ischemia-induced apoptosis in neurons. *J Neurosci* **19**: 3809-3817.

McAfoose J, Baune BT (2009) Evidence for a cytokine model of cognitive function. *Neurosci Biobehav Rev* **33**:355-366.

McGrath EE, Marriott HM, Lawrie A, Francis SE et al. and Whyte MK (2011) TNF-related apoptosis-inducing ligand (TRAIL) regulates inflammatory neutrophil apoptosis and enhances resolution of inflammation. *J Leukoc Biol* **90**: 855-865.

Muir KW, Tyrrell P, Sattar N, Warburton E (2007) Inflammation and ischaemic stroke. *Curr Opin Neurol* **20**: 334-342.

Nakajima T, Iwabuchi S, Miyazaki H, Okuma Y, et al. and Kawahara K (2004) Preconditioning prevents ischemia-induced neuronal death through persistent Akt activation in the penumbra region of the rat brain. *J Vet Med Sci* **66**: 521-527.

Negm OH, Mannsperger HA, McDermott EM, Drewe E et al. and Tighe PJ (2014) A pro-inflammatory signalome is constitutively activated by C33Y mutant TNF receptor 1 in TNF receptor-associated periodic syndrome (TRAPS). *Eur J Immunol* **44**: 2096-110.

Nitsch R, Bechmann I, Deisz RA, Haas D, Lehmann TN, Wendling U, Zipp F (2000) Human brain-cell death induced by tumour- necrosis-factor-related apoptosis-inducing ligand (TRAIL). *Lancet* **356**: 827-828.

Nocentini G, Cuzzocrea S, Genovese T, Bianchini R et al. and Riccardi C (2008) Glucocorticoid-induced tumor necrosis factor receptor-related (GITR)-Fc fusion protein inhibits GITR triggering and protects from the inflammatory response after spinal cord injury. *MolPharmacol* **73**: 1610-1621.

Oldenhuis CN, Stegehuis JH, Walenkamp AM, de

Jong S, de Vries EG (2008) Targeting TRAIL death receptors. *Curr Opin Pharmacol* **8**: 433-9.

Pace TW, Hu F, Miller AH (2007) Cytokine effects on glucocorticoid receptor function: relevance to glucocorticoid resistance and the pathophysiology and treatment of major depression. *Brain Behav Immun* **21**:9-19.

Papoff G, Hausler P, Eramo A, Pagano MG, Di Leve G, Signore A, Ruberti G (1999) Identification and characterization of a ligand-independent oligomerization domain in the extracellularregion of the CD95 death receptor. *J Biol Chem* **74**: 38241-50.

Park, KM, Bowers, WJ (2010) Tumor Necrosis Factor-alpha Mediated Signaling in Neuronal Homeostasis and Dysfunction, *Cell Signal* **22**: 977-983.

Pitti RM, Marsters SA, Ruppert S, Donahue CJ, Moore A, Ashkenazi A (1996) Induction of apoptosis by Apo-2 ligand, a new member of the tumor necrosis factor cytokine family. *J Biol Chem* **271**: 12687-12690.

Prat A, Biernacki K, Wosik K, Antel JP (2001) Glial cell influence on the human blood-brain barrier. *Glia* **36**: 145-155.

Ryan LA, Peng H, Erichsen DA, Huang Y et al. and Zheng J (2004) TNF-related apoptosis-inducing ligand mediates human neuronal apoptosis: links to HIV-1-associated dementia. *J Neuroimmunology* **148**: 127-139.

Schrimsher GW, Reier PJ (1992) Forelimb motor performance following cervical spinal cord contusion injury in the rat. *Exp Neurol* **117**: 287-298.

Secchiero P, Gonelli A, Carnevale E, Milani D, Pandolfi A, Zella D, Zauli G (2003) TRAIL promotes the survival and proliferation of primary human vascular endothelial cells by activating the Akt and ERK pathways. *Circulation* **107**: 2250-2256.

Secchiero P, Zerbinati C, Rimondi E, Corallini F et al. and Zauli G (2004) TRAIL promotes the survival, migration and proliferation of vascular smooth muscle cells. *Cell Mol Life Sci* **61**: 1965-1974.

Secchiero P, Melloni E, Corallini F, Beltrami AP et al. and Zauli G (2008) Tumor necrosis factor-related apoptosis-inducing ligand promotes migration of human bone marrow multipotent stromal cells. *Stem Cells* **26**: 2955-2963.

Shi Y (2004) Caspase activation, inhibition, and reactivation: a mechanistic view. *Protein Sci***13**: 1979-87.

Smyth MJ, Takeda K, Hayakawa Y, Peschon JJ, van den Brink MR, Yagita H (2003) Nature's TRAIL-on a path to cancer immunotherapy. *Immunity* **18**: 1-6.

Spierings DC, de Vries EG, Vellenga E, van den Heuvel FA et al. and de Jong S (2004) Tissue distribution of the death ligand TRAIL and its receptors. *J Histochem Cytochem* **52**: 821-31.

Takeda K, Smyth MJ, Cretney E, Hayakawa Y, Kayagaki N, Yagita H, Okumura K (2002) Critical role for tumor necrosis factor-related apoptosis-inducing ligand in immune surveillance against tumor development. *J Exp Med* **195**: 161-9.

Trauzold A, Siegmund D, Schniewind B, Sipos B et al. and Wajant H (2006) TRAIL promotes metastasis of human pancreatic ductal adenocarcinoma. *Oncogene* **25**: 7434-7439.

Uberti D, Cantarella G, Facchetti F, Cafici A, Grasso C, Bernardini R, Memo M (2004) TRAIL is expressed in the brain cells of Alzheimer's disease patients. *Neuro Report* **15**: 579-581.

Vilimanovich U, Bumbasirevic V (2008) TRAIL induces proliferation of human glioma cells by c-FLIPL-mediated activation of ERK1/2. *Cell Mol Life Sci* **65**: 814-826.

Voigt S, Philipp S, Davarnia P, Winoto-Morbach S et al. and Adam D (2014) TRAIL-induced programmed necrosis as a novel approach to eliminate tumor cells. *BMC Cancer* **14**: 74.

Walczak H, Haas TL (2008) Biochemical analysis of the native TRAIL death-inducing signaling complex. *Methods Mol Biol* **414**: 221-39.

Wang D, Liu D, Gao J, Liu M et al. and Zheng D (2013) TRAIL-induced miR-146a expression suppresses CXCR4-mediated human breast cancer migration. *FEBS J* **280**: 3340-3353.

Waterhouse NJ, Ricci JE, Green DR (2002) And all of a sudden it's over: mitochondrial outer-membrane permeabilization in apoptosis. *Biochimie* **3**: 113-21.

Wei W, Wang D, Shi J, Xiang Y et al. and Zheng D (2010) Tumor necrosis factor (TNF)-related apoptosis-inducing ligand (TRAIL) induces chemotactic migration of monocytes via a death receptor 4-mediated RhoGTPase pathway. *MolImmunol* **47**: 2475-2484.

Wiley SR, Schooley K, Smolak PJ, Din WS et al. and Goodwin RG (1995) Identification and characterization of a new member of the TNF family that induces apoptosis.

Immunity **3**: 673-682.

Wosik K, Biernacki K, Khouzam MP, Prat A (2007) Death receptor expression and function at the human blood brain barrier. *J NeurolSci* **2 59**: 53-60.

Wu GS, Burns TF, Zhan Y, Alnemri ES, El Deiry WS (1999) Molecular cloning and functional analysis of the mouse homologue of the KILLER/DR5 tumor necrosis factor-related apoptosis inducing ligand (TRAIL) death receptor. *Cancer Res* **59**: 2770-2775.

Yen ML, Hsu PN, Liao HJ, Lee BH, Tsai HF (2012) TRAF-6 dependent signaling pathway is essential for TNF-related apoptosis-inducing ligand (TRAIL) induces osteoclast differentiation. *PLoS ONE***7**: e38048.

Zhou DH, Yang LN, Roder C, Kalthoff H, Trauzold A (2013) TRAIL-induced expression of uPA and IL-8 strongly enhanced by overexpression of TRAF2 and Bcl-xL in pancreatic ductal adenocarcinoma cells. *Hepatobiliary Pancreat Dis Int* **12**: 94-98.

Zhu CB, Blakely RD, Hewlett WA (2006) The proinflammatory cytokines IL-1 beta and TNF-alpha activateserotonintransporters.*Neuropsychopharmacology* **31**: 2121-2131.

MICROGLIAL MICROVESICLES ALTER EXCITATION-INHIBITION BALANCE IN THE BRAIN

M. GABRIELLI[1] and C. VERDERIO[2,3]

[1]Department of Medical Biotechnology and Translational Medicine, University of Milano, Milano, Italy; [2]CNR Institute of Neuroscience, Milano, Italy; [3]IRCCS Humanitas, Rozzano (Milano), Italy

This brief congress report summarizes the oral communication held by Martina Gabrielli at the National Meeting of PhD Students in Neuroscience "New Perspectives in Neurosciences", which took place in Naples on February 26th, 2015. The presentation highlighted the role of extracellular vesicles (EVs) released from reactive microglia in the modulation of synaptic transmission. Special regard was given to novel evidence that microglial EVs carry on their surface active endocannabinoids (eCBs), thus serving as vehicles for their transport across the extracellular space.

In recent years extracellular vesicles (EVs) have become a major topic in neurobiology. Once regarded as mere artifacts, they are now considered very important mechanisms of cell-to-cell communication in the brain (Cocucci and Meldolesi, 2015; Fruhbeis et al. 2013), involved in a number of physiological and pathological processes (Nakano et al. 2015; Rajendran et al. 2014; Smith et al. 2015). EVs are membrane vesicles released by virtually all cell types and capable of transferring active molecules in a target-specific way. During biogenesis EVs enclose proteins, nucleic acids and lipids from donor cells and deliver these molecules to target cells by fusion or internalization (Cocucci and Meldolesi, 2015; Cocucci et al. 2009; Raposo and Stoorvogel, 2013; Tetta et al. 2013). EV composition may change, reflecting the activation state of parental cells (Cocucci and Meldolesi, 2011). Two kinds of EVs have been described to date: microvesicles (MVs) and exosomes. MVs shed directly from the plasma membrane; they are heterogeneous and quite large, ranging from 100 nm to 1 μM in diameter (Cocucci and Meldolesi, 2011; Mause and Weber, 2010; Raposo and Stoorvogel, 2013). Exosomes originate from the endocytic compartment; they are homogeneous and smaller, having a diameter of 40-100 nm (Mause and Weber, 2010; Raposo and Stoorvogel, 2013; Simons and Raposo, 2009). The two population of EVs have distinct features and may exert distinct functions, in spite of several overlapping roles (Cocucci and Meldolesi, 2015).

EVs released by microglia, the immune cells of the brain, has been widely studied (Prada et al. 2013). A few years ago we reported that primary cultured microglia release EVs upon stimulation with adenosine triphosphate (ATP) (Bianco et al. 2005). More specifically we demonstrated that ATP promotes release of MVs through activation of $P2X_7$ receptor (Bianco et al. 2009; Bianco et al. 2005). This ATP receptor responds to high concentration of extracellular ATP (Farber and Kettenmann, 2006; Lalo et al. 2011), a typical danger signal (Davalos et al. 2005; Fiebich et al. 2014). We then observed that ATP-induced MV production increases drastically

Key words: extracellular vesicles, microglia-neuron signaling, endocannabinoids, CB_1 receptor, sphingolipids, GABA release, glutamate release

Corresponding author: Martina Gabrielli
Department of Medical Biotechnology and Translational Medicine, (University of Milano) via Vanvitelli 32
20129, Milano, Italy
Tel.: +39 02 503 17009 Fax: +39 02 503 17132
e-mail: martina.gabrielli@unimi.it

2279-5855 (2015)

in reactive microglia, exposed to the endotoxin LPS or TH1 cytokines, which polarize microglia towards an inflammatory phenotype (Verderio et al. 2012). In addition, we provided evidence for the *in vivo* existence of microglial MVs: MVs positive for typical microglial markers were detected by electron microscopy and confocal microscopy in the cerebrospinal fluid (CSF) collected from rodents and humans (Verderio et al. 2012). Interestingly, MV production reflected the extent of microglial activation: the concentration of MVs increased in the CSF of mouse models of multiple sclerosis (mice with experimental autoimmune encephalomyelitis) at relapses and in the CSF of multiple sclerosis patients in the acute phase of the disease (Verderio et al. 2012). More importantly, our findings indicated that MVs released from reactive microglia contribute to neuroinflammation, as they propagate inflammatory signals, such as the pro-inflammatory cytokine IL-1beta, to other glial cells (Verderio et al. 2012).

Since microglia play a crucial role in homeostatic plasticity and influence neurotransmission under neuroinflammatory conditions (Centonze et al. 2009; Centonze et al. 2010; Kettenmann et al. 2011; Kettenmann et al. 2013; Parkhurst et al. 2013) we asked whether MVs may alter synaptic transmission. In this report we describe how we addressed this question and elucidated the molecular mechanisms by which microglial MVs modulate presynaptic functions.

MICROGLIAL MVs ALTER SYNAPTIC TRANSMISSION: *IN VIVO* PROOF-OF-PRINCIPLE

The first evidence supporting a role for microglial MVs in modulation of neurotransmission came from *in vivo* recordings of potentials evoked by visual stimuli following injection of microglial MVs into the rat visual cortex (Antonucci et al. 2012). Briefly, MVs were isolated by differential centrifugation from the supernatant of ATP-stimulated N9 microglial cells, and injected by a glass pipette into the visual cortex of anesthetized rats. Before and 1 h after injection of MVs in the vicinity of a recording electrode, visual evoked potentials (VEPs), and single units were recorded. By this approach we found that microglial MVs induce a significant increase in the amplitude of VEPs evoked by high contrast stimuli, which reflects the sum of excitatory currents elicited by sensory stimulation (Porciatti et al. 1999; Restani et al. 2009). In addition, we observed that MV injection causes an enlargement of neuron receptive fields, an alteration typically explained by an excitation-inhibition unbalance in the visual cortex (Benali et al. 2008; Liu et al. 2010). Thus, these experiments provided a proof-of-principle that microglial MVs are able to acutely alter synaptic transmission *in vivo*.

MICROGLIAL MVs ENHANCE EXCITATORY TRANSMISSION THROUGH STIMULATION OF THE SPHINGOLIPID CASCADE

Further *in vitro* experiments were performed on cultured rat hippocampal neurons in order to gain insight into the molecular mechanisms underlying synaptic modulation mediated by microglial MVs (Antonucci et al. 2012). Cultured neurons were incubated for 40-45 min with MVs from primary microglia, and neuronal activity was analyzed by whole-cell voltage-clamp electrophysiological recordings. First, we analyzed MV effects on excitatory synapses and found that MVs induce an increase in presynaptic release probability (Antonucci et al. 2012) (Fig. 1, left). This effect of MVs was indicated by recordings of spontaneous miniature excitatory postsynaptic currents (mEPSCs) and evoked glutamate transmission (eEPSCs), application of short-term plasticity protocols and analysis of responses to sucrose hypertonic solution. Notably, a similar enhancement of spontaneous electrical activity was induced by MVs derived from astrocytes (Antonucci et al. 2012) or exosomes produced by oligodendrocytes (Frohlich et al. 2014). This evidence indicates that EVs produced by distinct glial cell types share the capability to potentiate excitatory transmission.

Stimulation of glutamate exocytosis was a consequence of enhanced sphingolipid metabolism in response to microglial MVs (Antonucci et al. 2012). Indeed, biochemical analysis of sphingolipids in MV-treated neurons showed enhanced production of ceramide and sphingosine, while pharmacological blockade of sphingosine synthesis completely prevented the enhancement of glutamate transmission

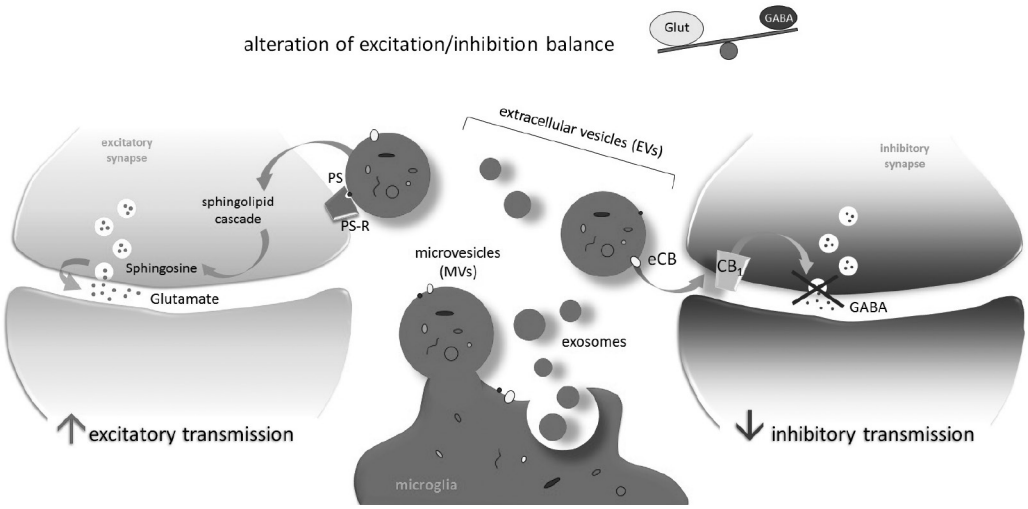

Fig. 1. ***Microglial microvesicles (MVs) induce excitation-inhibition unbalance.*** *Microglia release both types of extracellular vesicles (EVs): MVs and exosomes. Microglial MVs stimulate excitatory transmission (**left**) and, at the same time, depress inhibitory transmission (**right**), thus altering excitation-inhibition balance. (**left**) Microglial MVs act on excitatory presynaptic terminals, stimulating sphingolipid metabolism to produce the sphingolipid sphingosine. Sphingosine accounts for MV-mediated increase of glutamate release probability. This effect requires the contact of MVs with neuronal surface through interaction of phosphatidil-serine (PS) residues, exposed on the outer MV membrane, with specific PS-receptors (PS-R) on neurons. (**right**) Microglial MVs, carrying eCBs on their surface, inhibit GABAergic transmission by activating CB_1 receptors on presynaptic terminals of inhibitory interneurons.*

induced by MVs. Experiments performed on acid sphingomyelinase knock-out mice, which are impaired in sphingosine synthesis, corroborated these findings (Antonucci et al. 2012) (Fig. 1, left).

MICROGLIAL MVs CARRY ACTIVE ENDOCANNABINOIDS ON THEIR SURFACE

More recently, we investigated possible effects of MVs on inhibitory synapses. Analysis of miniature inhibitory postsynaptic currents (mIPSCs) showed a decrease in spontaneous GABA release in MV-treated neurons (Gabrielli et al. 2015) (Fig. 1, right).

Among agents known to modulate spontaneous GABA release there are endocannabinoids (eCBs) which are important signaling molecules produced by neurons in the postsynaptic compartment, and work retrogradely on presynaptic terminals to inhibit neurotransmitter release via activation of specific CB_1 receptors (CB_1) (Castillo et al. 2012; Harkany et al. 2008; Heifets and Castillo, 2009; Kano et al. 2009). eCBs are also released by glial cells, with microglia producing 20-fold the amount secreted by neurons in inflammatory conditions (Carrier et al. 2004; Stella, 2009; Walter et al. 2002; Walter et al. 2003). eCBs are highly hydrophobic molecules; to reach the presynaptic terminals, they move across the hydrophilic extracellular space. However, how this movement occurs has been highly debated (Alger and Kim, 2011; Maccarrone et al. 2010). We recently showed that microglial MVs may act as vehicles for the transfer of functional eCBs to neurons (Gabrielli et al. 2015). This evidence was supported by the finding that MVs contain strikingly higher levels of the eCB anandamide than donor microglia, as revealed by mass spectrometry. In addition, we showed that vesicular eCBs activate presynaptic CB_1 and inhibit GABA release (Gabrielli et al. 2015) (Fig. 1, right). The involvement of vesicular eCBs in the inhibition of GABA release was indicated by the ability of the CB_1 antagonist SR171416A to completely abolish the decrease in mIPSC frequency evoked by MVs (Gabrielli et al. 2015). SR171416A was also able to inhibit MVs-

induced phosphorylation of ERK (Gabrielli et al. 2015), which is known to occur downstream CB_1 activation (Dalton and Howlett, 2012). These data suggest that eCBs are carried on the surface of MVs, as they are able to activate presynaptic CB_1.

MICROGLIAL MVs SIGNAL TO EXCITATORY AND INHIBITORY TERMINALS BY DISTINCT MOLECULAR PATHWAYS

Further experiments, performed in the presence of pharmacological block of sphingolipid metabolism, clarified that the potentiation of excitatory transmission evoked by MVs did not cross-affect inhibitory transmission. Similarly, pharmacological block of eCB signaling showed that microglial MVs directly potentiate excitatory transmission, independently of modulation on the inhibitory tone (Gabrielli et al. 2015). This means that MVs activate distinct signaling pathways and deliver distinct messages, depending on the GABAergic or glutamatergic nature of recipient neurons. The opposite effects of MVs on glutamatergic and GABAergic synapses, may underlie the excitatory-inhibitory unbalance evoked by microglial MVs in the visual cortex (Fig. 1).

CONCLUSIONS

Microglia-derived MVs are important mechanisms of microglia-to-neuron communication, able to acutely modulate neurotransmission. Our *in vivo* and *in vitro* electrophysiological data indicate that MVs produced by reactive microglia alter the excitation-inhibition balance in favour of a general network excitation. Excessive glutamate release may lead to excitotoxicity, a process involved in a vast number of diseases characterized by neuroinflammation and microglial activation (Centonze et al. 2009; Centonze et al. 2010). However, we cannot exclude that microglia release MVs in response to deficit of neuronal activity, thus representing a homeostatic mechanism to restore synaptic transmission and to preserve physiological network condition in the brain.

ACKNOWLEDGEMENTS

This work was supported by FISM (2012/R/17) granted to Claudia Verderio. The authors are grateful to Michela Matteoli and Mauro Maccarrone for previous discussion, and to Flavia Antonucci for previous work.

REFERENCES

Alger BE, Kim J (2011) Supply and demand for endocannabinoids. *Trends Neurosci* **34:** 304-315

Antonucci F, Turola E, Riganti L, Caleo M et al. and Verderio C (2012) Microvesicles released from microglia stimulate synaptic activity via enhanced sphingolipid metabolism. *EMBO J* **31:** 1231-1240

Benali A, Weiler E, Benali Y, Dinse HR, Eysel UT (2008) Excitation and inhibition jointly regulate cortical reorganization in adult rats. *J Neurosci* **28:** 12284-12293

Bianco F, Perrotta C, Novellino L, Francolini M et al. and Verderio C (2009) Acid sphingomyelinase activity triggers microparticle release from glial cells. *EMBO J* **28:** 1043-1054

Bianco F, Pravettoni E, Colombo A, Schenk U, Moller T, Matteoli M, Verderio C (2005) Astrocyte-derived ATP induces vesicle shedding and IL-1 beta release from microglia. *J Immunol* **174:** 7268-7277

Carrier EJ, Kearn CS, Barkmeier AJ, Breese NM et al. and Hillard CJ (2004) Cultured rat microglial cells synthesize the endocannabinoid 2-arachidonylglycerol, which increases proliferation via a CB2 receptor-dependent mechanism. *Mol Pharmacol* **65:** 999-1007

Castillo PE, Younts TJ, Chavez AE, Hashimotodani Y (2012) Endocannabinoid signaling and synaptic function. *Neuron* **76:** 70-81

Centonze D, Muzio L, Rossi S, Cavasinni F et al. and Martino G (2009) Inflammation triggers synaptic alteration and degeneration in experimental autoimmune encephalomyelitis. *J Neurosci* **29:** 3442-3452

Centonze D, Muzio L, Rossi S, Furlan R, Bernardi G, Martino G (2010) The link between inflammation, synaptic transmission and neurodegeneration in multiple sclerosis. *Cell Death Differ* **17:** 1083-1091

Cocucci E, Meldolesi J (2011) Ectosomes. *Curr Biol* **21:** R940-941

Cocucci E, Meldolesi J (2015) Ectosomes and exosomes: shedding the confusion between extracellular vesicles. *Trends Cell Biol*

Cocucci E, Racchetti G, Meldolesi J (2009) Shedding microvesicles: artefacts no more. *Trends Cell Biol* **19:** 43-51

Dalton GD, Howlett AC (2012) Cannabinoid CB1 receptors transactivate multiple receptor tyrosine kinases and regulate serine/threonine kinases to activate ERK in neuronal cells. *Br J Pharmacol* **165:** 2497-2511

Davalos D, Grutzendler J, Yang G, Kim JV et al. and Gan WB (2005) ATP mediates rapid microglial response to local brain injury in vivo. *Nat Neurosci* **8:** 752-758

Farber K, Kettenmann H (2006) Purinergic signaling and microglia. *Pflugers Archiv : European journal of physiology* **452:** 615-621

Fiebich BL, Akter S, Akundi RS (2014) The two-hit hypothesis for neuroinflammation: role of exogenous ATP in modulating inflammation in the brain. *Frontiers in cellular neuroscience* **8:** 260

Frohlich D, Kuo WP, Fruhbeis C, Sun JJ et al. and Kramer-Albers EM (2014) Multifaceted effects of oligodendroglial exosomes on neurons: impact on neuronal firing rate, signal transduction and gene regulation. *Philosophical transactions of the Royal Society of London Series B, Biological sciences* **369**

Fruhbeis C, Frohlich D, Kuo WP, Kramer-Albers EM (2013) Extracellular vesicles as mediators of neuron-glia communication. *Frontiers in cellular neuroscience* **7:** 182

Gabrielli M, Battista N, Riganti L, Prada I et al. and Verderio C (2015) Active endocannabinoids are secreted on extracellular membrane vesicles. *EMBO reports* **16:** 213-220

Harkany T, Mackie K, Doherty P (2008) Wiring and firing neuronal networks: endocannabinoids take center stage. *Curr Opin Neurobiol* **18:** 338-345

Heifets BD, Castillo PE (2009) Endocannabinoid signaling and long-term synaptic plasticity. *Annu Rev Physiol* **71:** 283-306

Kano M, Ohno-Shosaku T, Hashimotodani Y, Uchigashima M, Watanabe M (2009) Endocannabinoid-mediated control of synaptic transmission. *Physiol Rev* **89:** 309-380

Kettenmann H, Hanisch UK, Noda M, Verkhratsky A (2011) Physiology of microglia. *Physiol Rev* **91:** 461-553

Kettenmann H, Kirchhoff F, Verkhratsky A (2013) Microglia: new roles for the synaptic stripper. *Neuron* **77:** 10-18

Lalo U, Verkhratsky A, Pankratov Y (2011) Ionotropic ATP receptors in neuronal-glial communication. *Seminars in cell & developmental biology* **22:** 220-228

Liu BH, Li P, Sun YJ, Li YT, Zhang LI, Tao HW (2010) Intervening inhibition underlies simple-cell receptive field structure in visual cortex. *Nat Neurosci* **13:** 89-96

Maccarrone M, Dainese E, Oddi S (2010) Intracellular trafficking of anandamide: new concepts for signaling. *Trends Biochem Sci* **35:** 601-608

Mause SF, Weber C (2010) Microparticles: protagonists of a novel communication network for intercellular information exchange. *Circulation research* **107:** 1047-1057

Nakano I, Garnier D, Minata M, Rak J (2015) Extracellular vesicles in the biology of brain tumour stem cells - Implications for inter-cellular communication, therapy and biomarker development. *Seminars in cell & developmental biology*

Parkhurst CN, Yang G, Ninan I, Savas JN et al. and Gan WB (2013) Microglia promote learning-dependent synapse formation through brain-derived neurotrophic factor. *Cell* **155:** 1596-1609

Porciatti V, Pizzorusso T, Maffei L (1999) The visual physiology of the wild type mouse determined with pattern VEPs. *Vision research* **39:** 3071-3081

Prada I, Furlan R, Matteoli M, Verderio C (2013) Classical and unconventional pathways of vesicular release in microglia. *Glia* **61:** 1003-1017

Rajendran L, Bali J, Barr MM, Court FA et al. and Breakefield XO (2014) Emerging roles of extracellular vesicles in the nervous system. *J Neurosci* **34:** 15482-15489

Raposo G, Stoorvogel W (2013) Extracellular vesicles: exosomes, microvesicles, and friends. *The Journal of cell biology* **200:** 373-383

Restani L, Cerri C, Pietrasanta M, Gianfranceschi L, Maffei L, Caleo M (2009) Functional masking of deprived eye responses by callosal input during ocular dominance plasticity. *Neuron* **64:** 707-718

Simons M, Raposo G (2009) Exosomes--vesicular carriers for intercellular communication. *Curr Opin Cell Biol* **21:** 575-581

Smith JA, Leonardi T, Huang B, Iraci N, Vega B, Pluchino S (2015) Extracellular vesicles and their synthetic analogues in aging and age-associated brain

diseases. *Biogerontology* **16:** 147-185

Stella N (2009) Endocannabinoid signaling in microglial cells. *Neuropharmacology* **56 Suppl 1:** 244-253

Tetta C, Ghigo E, Silengo L, Deregibus MC, Camussi G (2013) Extracellular vesicles as an emerging mechanism of cell-to-cell communication. *Endocrine* **44:** 11-19

Verderio C, Muzio L, Turola E, Bergami A et al. and Furlan R (2012) Myeloid microvesicles are a marker and therapeutic target for neuroinflammation. *Ann Neurol* **72:** 610-624

Walter L, Franklin A, Witting A, Moller T, Stella N (2002) Astrocytes in culture produce anandamide and other acylethanolamides. *J Biol Chem* **277:** 20869-20876

Walter L, Franklin A, Witting A, Wade C et al. and Stella N (2003) Nonpsychotropic cannabinoid receptors regulate microglial cell migration. *J Neurosci* **23:** 1398-1405

INFLAMMATORY AND MORPHOLOGICAL CHARACTERIZATION OF A FOREIGN BODY RETINAL RESPONSE

M. DI PAOLO[1], D. GHEZZI[2], M.R. ANTOGNAZZA[3], M. METE[4], G. FREDDI[5], I. DONELLI[5], R. MACCARONE[1], G. PERTILE[4], G. LANZANI[3], F. BENFENATI[2] and S. BISTI[1]

[1]Department of Biotechnology and Applied Clinical Science, University of L'Aquila, Italy; [2]Department of Neuroscience and Brain Technologies, Istituto Italiano di Tecnologia, Genoa, Italy; [3]Center for Nano Science and Technology, Istituto Italiano di Tecnologia, Milan, Italy; [4]Ohpthalmology Operative Unit, Ospedale Sacro Cuore - Don Calabria, Negrar, Italy; [5]Innovhub-SSI, Silk Division, Milan, Italy

Substitutive strategies are promising approaches to apply when retinal diseases lead to total blindness. The first test to be performed is an *in-vivo* biocompatibility study. We evaluated tissue reactions following sub-retinal implantation of a foreign body. Experiments were performed on Royal College of Surgeons non-dystrophic congenic rats (RCS-rdy). Two-three-month-old animals were implanted with a piece of silk and left them to recover for at least 3 weeks before starting the experimental protocol. Immunofluorescence assays were performed in both implanted and non-implanted rats to verify the correct position of the prosthesis and its long-term tolerability. The expression of inflammatory markers was monitored on retinas (GFAP) after implantation. Results suggest a good tolerability of the foreign body. Morphological analysis of implanted eye confirmed that the silk did not seriously alter the structure of the healthy retina. Immuno-inflammation markers indicated a modest inflammatory reaction and suggested long-term tolerability. In conclusion, our results confirm the viability of silk as support of sub-retinal prosthesis as silk does not induce adverse reactions.

Retinal degenerative diseases, such as age-related macular degeneration (AMD) and *Retinitis pigmentosa* (RP), are the leading cause of photoreceptor lost and blindness in adults (Coleman et al. 2008; Curcio et al. 1996; Liu et al. 2015). Restoration of visual perception is one of the new frontiers for prosthetic devices that have great potentiality in coping with these devastating disorders. The preferential targets for implanting sub-retinal visual prostheses are diseases affecting retinal pigment epithelium and photoreceptors but preserving, at least partially, inner retinal layers (Light et al. 2014; Maghami et al. 2014). These devices have to be associated with a physical support as biocompatible as possible to maintain correct function and position. We evaluated the amount of retinal reaction against a possible biological scaffold for retinal prostheses, silk fibroin.

MATERIALS AND METHODS

Preparation of silk

Bombyx mori cocoons were supplied by CRA, Council of Research and Experiments in Agriculture, Apiculture and Sericulture Unit, Padua, Italy. Lithium bromide (LiBr) extra pure was obtained from Merck. Dialysis tubing

Key words: retina, silk, biocompatibility, visual prosthesis

Corresponding author:
M. Di Paolo,
Via Tiburtina Valeria n° 102,
65128, Pescara, Italy
Tel.: +39 3206729342; +44 7732580154
e-mail: mattiadipaolo@gmail.com

2279-5855 (2015)

cellulose membrane (MW cut-off = 12,000 Da) were obtained from Sigma Aldrich. Cocoons were degummed in autoclave at 120°C for 15' and then rinsed with distilled water to remove sericin. After room temperature drying and storage under controlled conditions (T = 20±2°C and relative humidity = 65±2%), SF fibres were dissolved in a 9.3M LiBr aqueous solution (T = 60±2°C, t = 3 h) to obtain a 10% w/v SF solution. The solution was then diluted with distilled water to obtain a 2% w/v SF solution and dialyzed against distilled water for 3 days using dialysis tubing cellulose membrane to remove LiBr salt. SF films were prepared by pouring 22.5 ml of SF solution into Teflon Petri Dishes (ø = 75 mm), followed by casting under fume hood at room temperature until complete solvent evaporation and thermal drying at 105°C for 20 h.

Animal care and surgical procedures

Royal College of Surgery non-dystrophic congenic animals (RCS-rdy/LAV) (UCSF School of Medicine San Francisco, California) were housed in standard conditions with *ad libitum* access to food and water under a 12/12-hour light/dark cycle. All animal manipulations and procedures were performed in accordance with the guidelines established by the European Community Council (Directive 2012/63/EU of 22 September 2010) and were approved by the Italian Ministry of Health.

Animals were implanted at mean age of 85 days in the right eye and the experimental protocol started two weeks after surgery. Ketamine/xylazine anaesthesia was used with intra peritoneal injection of 100 mg/kg ketamine, 12 mg/kg xylazine (Ketavet 100 mg/ml, Intervet production srl; Xylazine 1 g, Sigma Co.). Sub-retinal implantation technique was previously described by other groups (Butterwick et al. 2009). Briefly, a 1.5 mm incision was made through the sclera and choroid, 1.5 mm posterior to the limbus and the implant was placed into the sub-retinal space using a custom-made implantation tool. The sclera and conjunctiva were electrocautery sutured.

Five animals were used in each group. Implanted eyes were compared with the fellow eye (internal control group) and healthy control group.

Preparation of explanted retinas

The superior aspect of the eye was marked with an indelible marker by a stitch in the conjunctiva, after euthanasia with CO2. Thereafter, the eyes were dissected free and fixed by immersion in 4% paraformaldehyde fixative buffer at 4°C for 1 h. After three rinses in 0.1 M phosphate-buffered saline (PBS), eyes were left overnight in a 15% sucrose solution to provide cryoprotection. Eyes were embedded in mounting medium (Tissue Tek OCT compound; Sakura Finetek, Torrance, CA) by snap freezing in liquid nitrogen. Cryosections were cut at 20 µm (CM1850 Cryostat; Leica, Wetzlar, Germany) with the eyes oriented so that the sections extended from superior to inferior edge. Sections were mounted on gelatin and poly-L-lysine-coated slides and were then dried overnight in 50°C oven and stored at −20°C until processed.

Immunohistochemistry: Iba1 and GFAP staining

Retinal sections were washed with 0.1 M PBS (twice for 10 min) and incubated in 10% normal goat serum in 0.1 M PBS for 1 h at room temperature, to block non-specific binding. Sections were then incubated overnight at 4°C with primary antibodies (rabbit polyclonal anti GFAP 1:700, DakoCytomation, Campbellfield, Australia; mouse polyclonal anti Iba1, 1:200). After 3 rinses in PBS for 10 min each, sections were incubated with an appropriate secondary antibody (1:1,000 ALEXA Fluor 594, 1:200 ALEXA Fluor 488; Molecular Probes, Invitrogen Carlsbad, CA), for 1 h at 37°C. This was followed by three 5-min washes in PBS and counterstaining with DNA-specific label, bisbenzamide (Hoechst) 1:10,000, for 1 min at room temperature (RT) to measure the thickness of the photoreceptor layer (Valter et al. 2005). Images were taken by confocal microscope (Nikon, Tokyo, Japan) and fluorescence microscope (Nikon). The spatial resolution employed was 1,024 × 1,024, the pinhole was set at 1 airy unit (AU) and Z stacks were made with 17 pictures and all stacks were collected using a x40 objective. Final images of all groups were processed in parallel using Adobe Photoshop CS5 software (Adobe Systems Inc., San Jose, CA, USA). Outer nuclear layer (ONL) thickness was measured starting at the dorsal edge along the vertical meridian crossing the optic nerve head according to a procedure already described. Measurements were reported at 1-mm intervals (each point was the mean of four measurements at 250-µm intervals). In each retina, we measured two sections. We measured the pixel intensity of GFAP expression of Müller cells along retinal sections, from the superior to the inferior edge.

Outcome measures

Three criteria of neuroreaction were used, the surviving population of photoreceptors, the rate of microglial activation with Iba1+ cells counting and the expression of the stress-inducible protein GFAP in Müller cells (Gallego et al. 2012; Noailles et al. 2014).

Statistical analysis

The significance of differences in ONL thickness, Iba1+ cells counting and GFAP labeling associated with conditioning were assessed using ANOVA, followed by the multiple comparison Tukey's test. Results are expressed as the mean ± SEM; $p < 0.05$ was considered significant.

RESULTS

Morphological analysis: photoreceptor survival

Fig. 1A shows a representative reconstruction of vertical section of implanted retina with a bisbenzimide labeling. The correct position of the silk implant was maintained with a good preservation of the ONL.

The result is shown quantitatively in Fig. 1B which illustrates ONL thickness in healthy control, implanted eye and internal control as a function of distance between the inferior and superior edges of the retina. ONL thinning induced by silk is relevant only at the retina-silk interface in the superior retina (1st point superior retina: One way ANOVA,* p<0.05; Tukey's test, implanted eye *vs* internal control p=0.739; implanted eye *vs* healthy retina p<0.05; internal control *vs* healthy retina p=0.092—2nd point superior retina: One way ANOVA, *p<0.05; Tukey's test, implanted eye *vs* internal control p<0.05; implanted eye *vs* healthy retina p<0.05; internal control *vs* healthy retina p=0.162— 3rd point superior retina: One way ANOVA, ***p<0.0001; Tukey's test, implanted eye *vs* internal control p<0.001; implanted eye *vs* healthy retina p<0.0001; internal control *vs* healthy retina p=0.428 — 4th point superior retina: One way ANOVA,*** p<0.001; Tukey's test, implanted eye *vs* internal control p<0.05; implanted eye *vs* healthy retina p<0.001; internal control *vs* healthy retina p=0.063).

Fig. 1C shows mean ONL thickness averaged

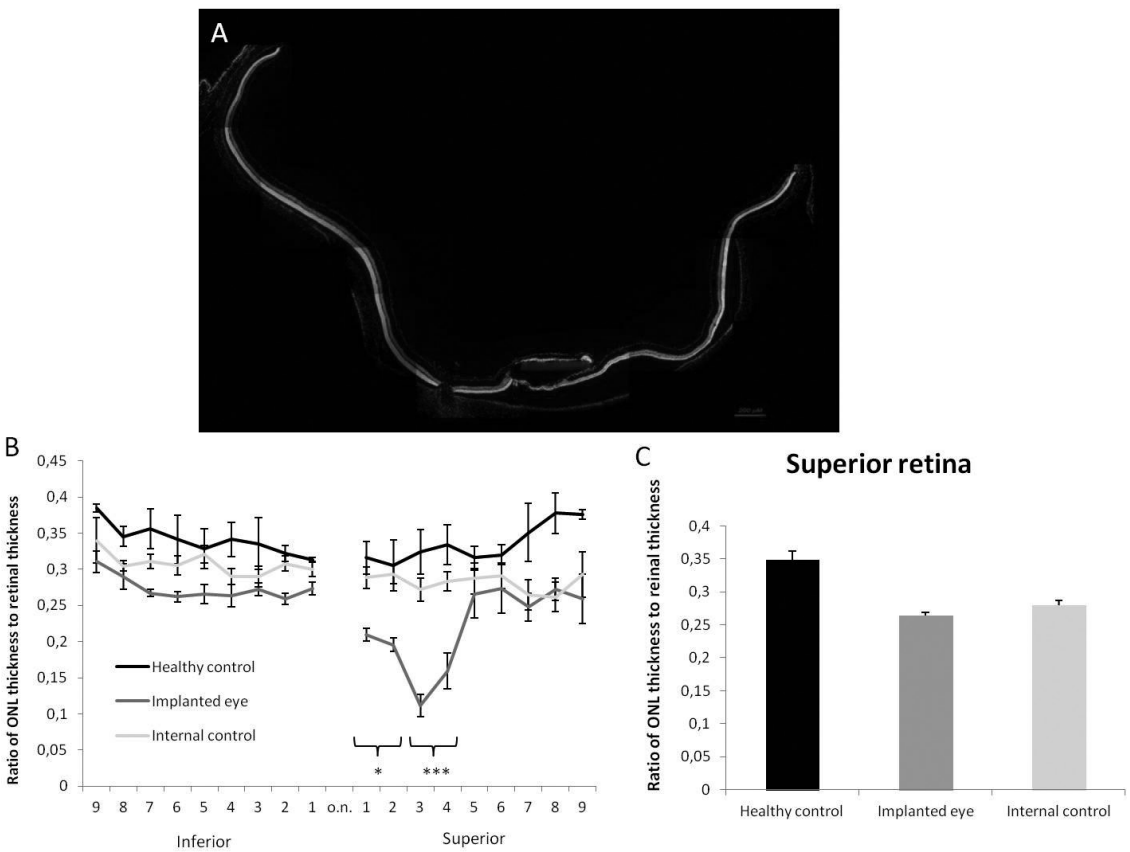

Fig. 1. *Impact of the silk presence on the thickness of the ONL superior retina.* ***A)*** *Reconstruction of vertical section of implanted retina with bisbenzimide labeling. Note the position of the silk under the retina 2 months after surgical insertion of silk.* ***B)*** *Ratio of ONL thickness to retinal thickness, from the superior to the inferior edge through the optic disc (O.D.).* ***C)*** *Ratio of ONL thickness to retinal thickness, in the non-implanted superior area (the superior retinal area without a silk-retina interface). No significant differences among the three groups, p=0.460.*

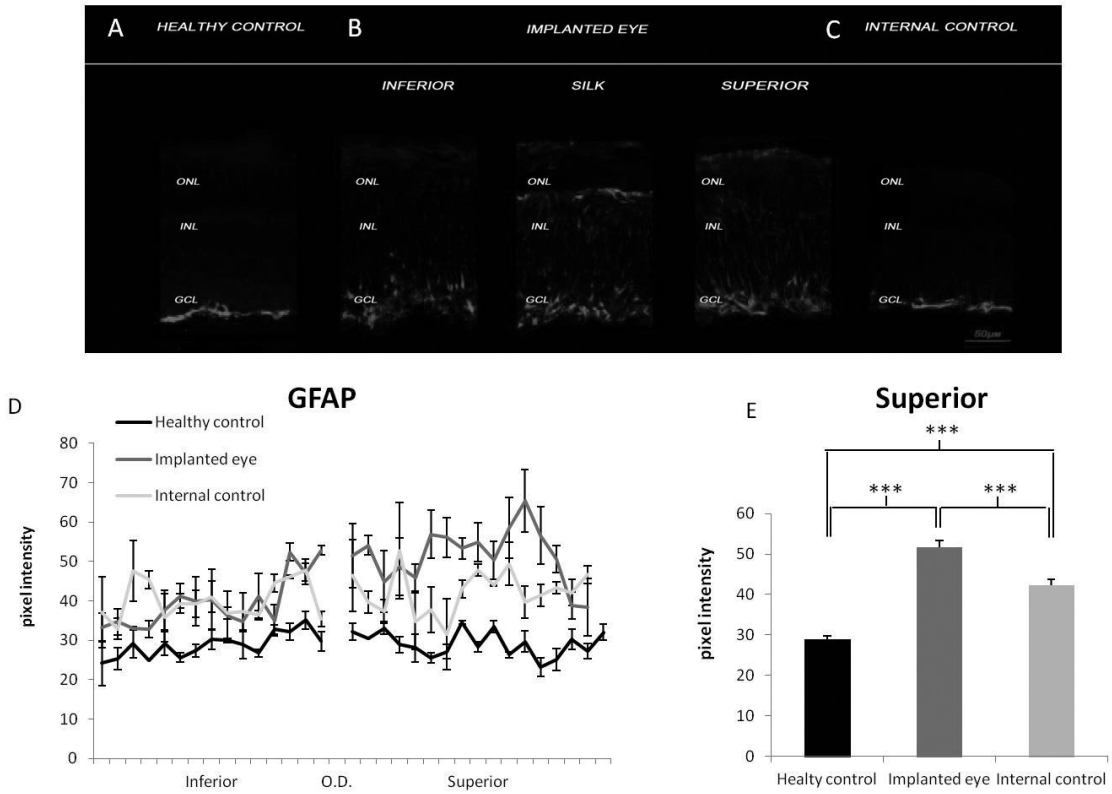

Fig. 2. *Impact of silk presence on GFAP labeling of Müller cells A–C. Representative GFAP labeling in healthy control (**A**), implanted eye (**B**), internal control (**C**) 2 months after surgical insertion of silk. Surgery and silk presence induced the up-regulation of GFAP in the radially oriented Müller cells; the protein is visible along the full length of the Müller cells, from the ILM to the OLM. **D**) Quantification of GFAP expression as a function of distance from superior edge through the optic disc (O.D.). **E**) Mean GFAP expression in the non-implanted superior area (the superior retinal area without a silk-retina interface). The difference among the groups is statistically significant.(One way ANOVA, ***p < 0.001; Tukey's test, implanted eye vs internal control ***p<0.001 implanted eye vs healthy retina ***p<0.001 internal control vs healthy retina ***p<0.001).*

across superior retina, in all experimental groups. The comparison was made by measuring ONL thickness in retinal fields without a silk-retina interface. The difference among the groups is not statistically significant (p=0.460).

Inflammatory marker: impact on GFAP expression

Fig. 2 shows representative images of GFAP expression in the superior retina, in the various experimental groups. In controls, GFAP expression is confined to the astrocytes at the inner surface of the retina (Fig. 2A). Surgical operation and the presence of the silk implant induce a significant up-regulation of GFAP in the radially oriented Müller cells compared to the internal control (Fig. 2C); the protein was visible in Müller cells at the level of the silk implant and in the inferior and superior sides (Fig. 2B).

The result is shown quantitatively in Fig. 2 D, E. The Müller cell labeling was consistent along the superior retina. The difference in the GFAP expression was significant between internal control and implanted group (***p<0.001; Fig. 3E).

Immune response: microglia activation

Fig. 3 shows representative images of activated microglia (Iba1 staining) in the superior retina, in all experimental groups. In control, microglia is located

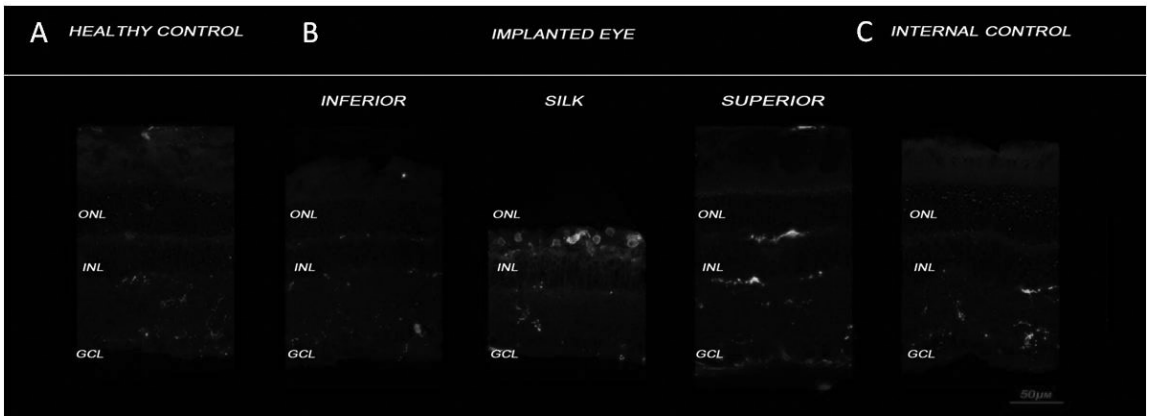

Fig. 3. *Distribution and morphology of microglia activated in (**A**) healthy control, (**B**) implanted eye and (**C**) internal control. Vertical section of the central retina immunolabeled with Iba1. Note presence maximum of Iba1+ cells in correspondence of the silk implant 2 months after implantation.*

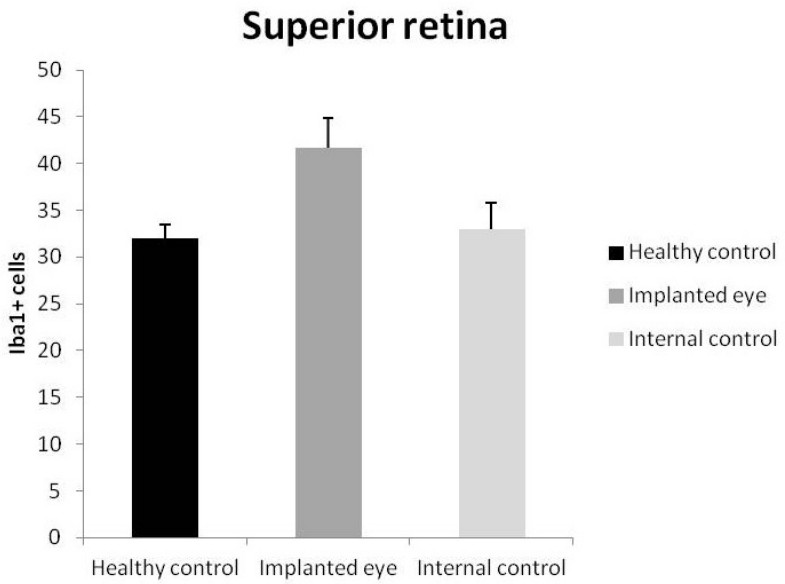

Fig. 4. *Quantification of microglia activated in the healthy control, implanted eye and internal control. Counts of Iba1+ cells in all retinal layers in the portion central superior of the non-implanted superior area (the central superior retinal area without a silk-retina interface). The implanted eye group and the internal control group values were not significantly different (One way ANOVA, $p > 0.273$).*

in the inner retina (Fig. 3A). Surgical operation and the silk implant produced a microglial activation defined by morphological changes and focal migration (Noailles et al. 2014) in the retina at the level of the implant (Fig. 3B).

The result is shown quantitatively in Fig. 4. IBA1+ cells were counted along the superior retina, without considering silk-retina interface, in the various experimental groups. The difference in the amount of labeled microglial cells, between internal

control and implanted group, was not significant (One way ANOVA $p > 0.273$).

DISCUSSION

Our results show that two months after surgical insertion of a silk-based substrate, the morphology of the retina was highly preserved, suggesting a high level of biocompatibility. As consequence of a low rate of neural cell death, the outer nuclear layer remains of normal thickness, except for a small area close to the implanted silk. As expected, a marked increase in GFAP expression was present in the operated eye, suggestive of an inflammatory response that was not, however, so intense as to induce a significant microglia activation. Altogether our data support silk as a good candidate biomaterial to support retinal visual prosthesis implants.

ACKNOWLEDGEMENTS

Supported by Telethon grant GP12033.

REFERENCES

Butterwick A, Huie P, Jones BW, Marc RE, Marmor M, Palanker D. (2009) Effect of shape and coating of a subretinal prosthesis on its integration with the retina. *Exp Eye Res* **88**(1):22–9.

Coleman RH, Chan CC, Ferris FL, III, and Chew EY (2008) Age-related macular degeneration *Lancet* **372**(9652): 1835–1845.

Curcio CA, Medeiros NE, Millican CL (1996) Photoreceptor loss in age-related macular degeneration. *Invest Ophthalmol Vis Sci* **37**: 1236–1249.

Gallego BI, Salazar JJ, Hoz R, Rojas B, Ramírez AI, Salinas-Navarro M, Ortín-Martínez A , Valiente-Soriano FJ , Avilés-Trigueros M , Villegas-Perez MP, Vidal-Sanz M, Triviño A, Ramírez JM (2012) IOP induces upregulation of GFAP and MHC-II and microglia reactivity in mice retina contralateral to experimental glaucoma. *J Neuroinflammation* **9**:92

Light JG, Fransen JW, Adekunle AN, Adkins A, Pangeni G, Loudin J, Mathieson K, Palanker DV, McCall MA, Pardue MT (2014) Inner retinal preservation in rat models of retinal degeneration implanted with subretinal photovoltaic arrays. *Exp Eye Res* **128**:34-42

Liu X, Zhang Y, He Y, Zhao J, Su G (2015) Progress in histopathologic and pathogenesis research in a retinitis pigmentosa model. *Histol Histopathol.* **11**:11596.

Maghami MH, Sodagar AM, Lashay A, Riazi-Esfahani H, Riazi-Esfahani M Visual prostheses: the **enabling technology** to **give sight** to the **blind (2014)** *J Ophthalmic Vis Res* **9(4)**:494-505.

Noailles A, Fernández-Sánchez L, Lax P, Cuenca N (2014) Microglia activation in a model of retinal degeneration and TUDCA neuroprotective effects. *J. Neuroinflammation* **11**: 186.

Valter K, Bisti S, Gargini C, Di Loreto S, Maccarone R, Cervetto L, Stone J (2005) Timecourse of neurotrophic factor upregulation and retinal protection against light damage following optic nerve section. *Invest Ophthalmol Vis Sci* **46**:1748–175.

INNOVATIVE ROBOTIC AND AUTOMATED TOOLS FOR ASSESSMENT OF MOTOR RECOVERY IN STROKE MOUSE MODELS

C. ALIA[1,2], C. SPALLETTI[1,3], S. LAI[4], A. PANARESE[1,4], S. MICERA[4,5] and M. CALEO[1]

[1]CNR Neuroscience Institute, Pisa, Italy; [2]Scuola Normale Superiore, Pisa, Italy; [3]Istituto di Scienze della Vita, Scuola Superiore Sant'Anna, Pisa, Italy; [4]Neural Engineering Area, The BioRobotics Institute, Scuola Superiore Sant'Anna, Pisa, Italy; [5]Bertarelli Foundation Chair in Translational NeuroEngineering Laboratory, Center for Neuroprosthetics, Swiss Federal Institute of Technology, Lausanne, Switzerland

Post-stroke motor rehabilitation has been extensively studied for many years, but the neurophysiological mechanisms of recovery remain incompletely understood. Moreover, key questions on whether restoration of function occurs via compensation and "true recovery" remain to be answered. Here, we summarize data in the literature and two recent studies from our group describing innovative tools for evaluating post-stroke forelimb motor deficits in mouse models. The first part describes a robotic platform for measuring and training forelimb function after stroke. Kinetic and kinematic parameters during the robot-mediated retraction task efficiently detect the post-stroke motor deficit. In addition, training on the platform has beneficial effects on motor function. The second part shows the implementation of a semi-automated tool to study pre- and post-stroke forelimb kinematics during the single pellet reaching task. This tool effectively reveals the use of compensatory strategies even after partial recovery in end-point measures (i.e. the number of correct grasps). We finally discuss the benefit of using these innovative tools to design and test novel rehabilitative strategies, aimed at improving post-stroke motor function, by combining motor training with modulation of spontaneous neuroplasticity.

Stroke is one of the leading causes of death and is the main origin of adult disability. When an ischemic insult occurs in the motor cortex, one or more body parts contralateral to the infarct result impaired or paretic. The degree of the motor impairment depends on many factors such as the extent of the infarct, the identity of the damaged region and the effectiveness of the initial neuroprotective interventions. Once neuroprotective therapies have been applied and the extent of the damage has been stabilized, the only chance for improving motor function is a motor rehabilitation therapy.

Many clinical issues are still open, such as the timing of the intervention, the type and the intensity of rehabilitation. Regarding rehabilitative approaches, robotic rehabilitation has been introduced in clinical practice in recent years, in addition to conventional physiotherapy (Krebs & Hogan, 2006). The main benefits of robotic rehabilitation are the high repeatability, the possibility to perform a greater number of exercises in a single session and the high intensity of task-oriented training (Posteraro et al., 2009). Moreover, robotic devices allow for several kinetic and kinematic measures in terms of forces exerted, and precision and smoothness of the movement that offer a more quantitative evaluation of

Key words: reaching, stroke, mice, robotic rehabilitation, motor recovery

Corresponding author:
Claudia Alia,
Istituto di Neuroscienze – CNR,
via Moruzzi 1, 56124 Pisa, Italy
Tel.: +39 050 3153189
e-mail: alia@in.cnr.it

2279-5855 (2015)

the motor performance compared with the traditional methods, i.e. qualitative clinical scales (Sicuri et al., 2014). Indeed, these robots incorporate sensory components, allowing for a complete feedback and monitoring of the therapy progress over time, even adjusting the degree of the robot assistance based on the progress of each patient.

Most clinical and pre-clinical studies on rehabilitation have been focused on the upper limb function, since a serious disability of the upper limb can affect the performance of several daily living activities (Aisen et al., 1997; Brewer et al., 2013; Fasoli et al., 2003; Volpe et al., 2000). Furthermore, studying the upper limb allows a quite simple monitoring of the longitudinal recovery, although innovative tools are required to better understand mechanisms underlying the motor function recovery.

The main target of motor rehabilitation is to allow patients to recover the lost function. Rehabilitation therapy trains the affected limb with specific exercises, with the aim of also improving performance of daily activities where the movement of the limb is necessary (i.e., generalization). For example, it is desirable that after a specific goal-directed grasping rehabilitation in a stroke patient, the subject improves the capability in i.e. grasping a glass of water. To evaluate the overall proficiency in this task, the end-point measure would be the number of correctly grasped glasses. However, the motor strategy used to grasp the glass could be changed after post-stroke rehabilitation, compared to the pre-stroke movement. This phenomenon is called compensation (Kitago et al., 2013; Zangwill, 1947) and includes all the changes in motor strategy involving the relative joint timing- and spatial coordination. In this context, kinematics is a potent tool to discriminate between post-stroke "true recovery" and compensatory strategies, making it useful also in pre-clinical studies in order to discriminate between maladaptive and adaptive recovery-driven neuroplasticity.

In this context, studies on animal models are convenient since they allow us to perform combined behavioral, molecular and mechanistic investigations. In particular, mice are largely used in this field because of their convenience in terms of costs, reproducibility, manageability and the broad-spectrum of investigations (Ginsberg & Busto, 1989). Moreover, rodents are able to perform forelimb movement partially comparable to humans such as grasping and reaching movements (Klein et al., 2012). Due to these similarities, some recent studies investigated the kinetics and kinematics of forelimb movements in stroke mice models in order to compare these common impairment and recovery features in mice and humans (Braun et al., 2012; Sacrey et al., 2009). Particularly suitable for kinematics studies is the computing of the reaching movement trajectory for the following reasons: (i) it is an essential movement in humans; (ii) it is quite innate and spontaneous in rodents; (iii) it is conserved and stereotyped among subjects (both humans and mice).

In two of our recent papers (Lai et al., 2015; Spalletti et al., 2014), we characterized two innovative devices for the training and the evaluation of the mouse post-stroke forelimb function, considering also kinematic and kinetic parameters. Here, we summarize the main features of these tools and their usefulness for better understanding the mechanisms underlying post-stroke motor recovery.

ROBOTIC DEVICE FOR TRAINING AND MEASURING FORELIMB FUNCTION

In the last few years, many papers have focused on rehabilitation in stroke animal models, introducing post-stroke rehabilitative strategies that in many cases consist of modifications of the Skilled Reaching Task (see next section). Robotic rehabilitative approaches could overcome the limitation of the conventional human rehabilitation, which might be not fully effective because of the dependency on motivational issues of the patient and the difficulty to apply consistent and repeatable training. In our paper (Spalletti et al., 2014) we implemented an innovative robotic platform to rehabilitate post-stroke forelimb function using a robot-based protocol, that allows us to measure and monitor the forelimb progress over time.

Briefly, the robotic system is composed of a linear actuator, a 6-axis load cell, a precision linear slide and a custom-designed handle that was fastened to the mouse forelimb. Animals were head-fixed and kept in a U-shaped restrainer during the task on the device (Fig. 1). The robotic task

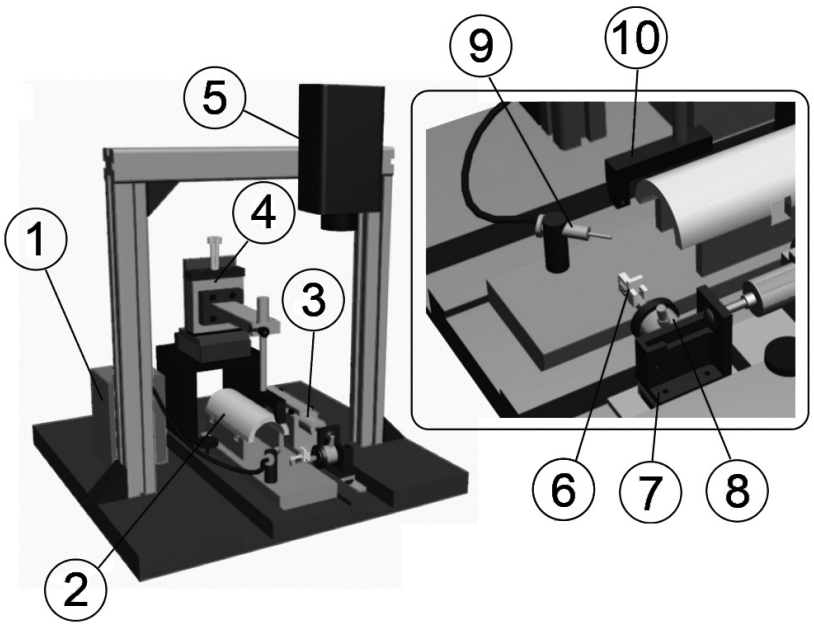

Fig. 1. *Schematic of the robotic platform. It consists of a peristaltic pump for liquid reward delivery (1), mouse restrainer (2), linear actuator (3), micromanipulator (4) for precise positioning of the mouse head, camera (5), handle (6), slide (7), load cell (8), gavage-feeding needle (9), and head fixation system (10).*

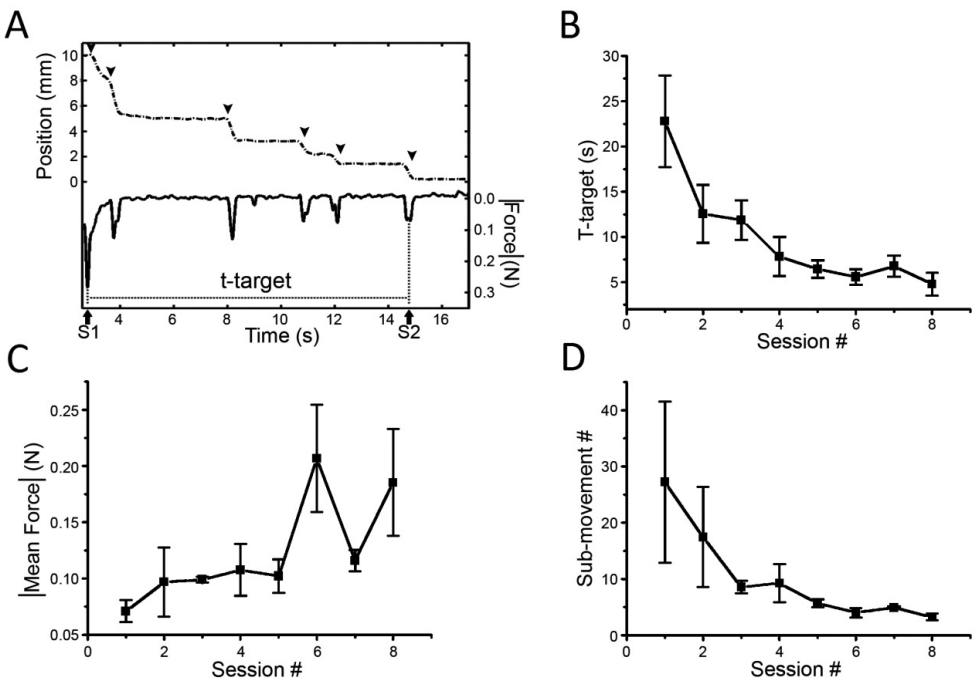

Fig. 2. ***A)*** *Representative example of a single retraction task (active phase) in the robotic platform. Dotted line, position of the handle over time; continuous line, force over time. S1 and S2, tones indicating begin and end task. The offset of the force profile at S1 was because of the opposing force exerted by the animal during extension by the actuator. Arrowheads indicate single sub-movements; note force peaks in correspondence of each sub-movement. T-target was calculated as time S2 − time S1. Variation of t-target (**B**), mean force exerted (**C**), and number of sub-movements (**D**) over the training sessions. Data are mean ± standard error.*

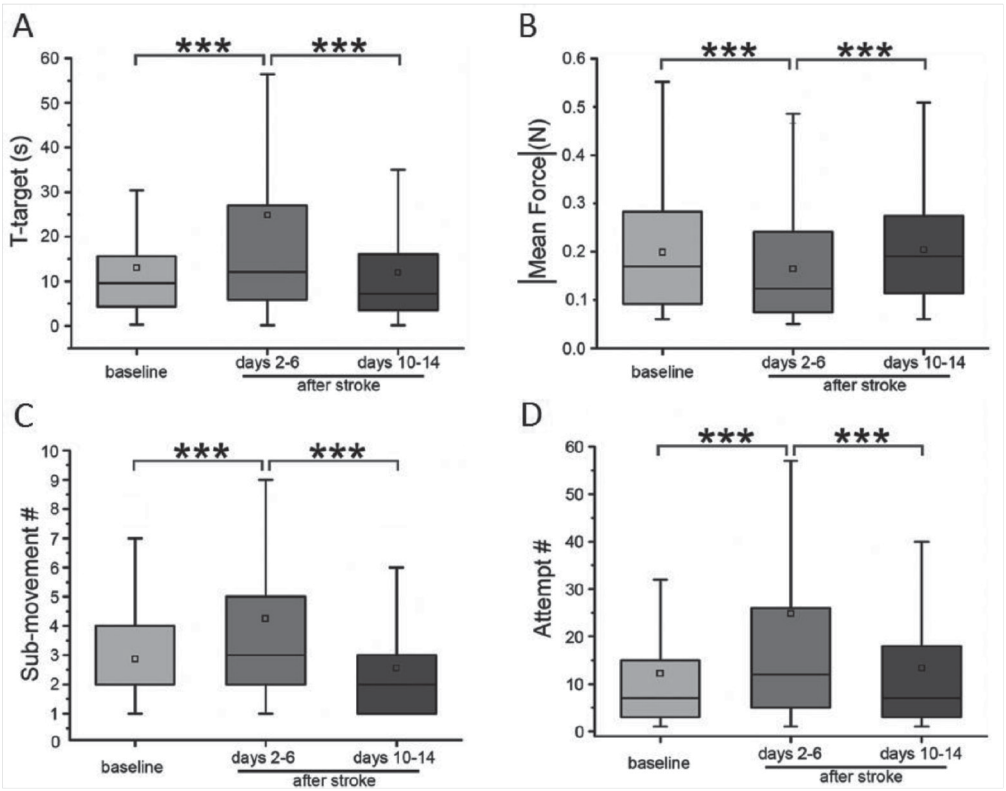

Fig. 3. *The robotic platform efficiently detects deficits and improvement of forelimb flexor performance following stroke. T-target (**A**), mean force exerted (**B**), number of sub-movements (**C**), and number of attempts (**D**) in baseline (pre-lesion) condition and either 2 to 6 days or 10 to 14 days after stroke. All animals were tested every other day in the robotic platform. Note the return to prelesion values of all parameters at the end of the training. Data are summarized by a box chart, in which the horizontal lines denote the 25th, 50th, and 75th percentile values, and the error bars denote the 5th and 95th percentile values; the square indicates the mean of the data set. ***P < 0.001 (Friedman test, P <0.001, followed by Dunn's post hoc test).*

consisted of a planar retraction movement: for each trial the actuator pushed the handle extending the mouse forelimb; from this position animals had to retract the forelimb to reach the starting position in order to receive a liquid reward. A video camera monitored the handle position during the task. Moreover, forces were recorded by the load cell and thus it was possible to align the position trace with the force curve. From these collected data the system automatically computed several parameters: (i) the time to accomplish the task (t-target); (ii) the number of sub-movements, defined as a force peak concomitant to a step in the position trace; (iii) the number of attempts, defined as a force peak not related to a position step (i.e. when the applied force does not overcome the static friction); (iv) the mean force exerted during the trial (Fig. 2A).

Firstly, we verified the learning of the robot-mediated task in a subset of healthy, naive animals. Within a few days, the animals learned to accomplish the retraction task, showing a consistent decrease in the t-target and in number of sub-movements. Simultaneously, we observed a consistent increase in the mean force exerted (Fig. 2B-D). Threfore, the robotic platform is an efficient tool to accurately measure forelimb performance during the learning phase of a new motor task.

To assess whether the robotic platform could detect stroke-induced motor deficits, we caused a local ischemic lesion in the Caudal Forelimb

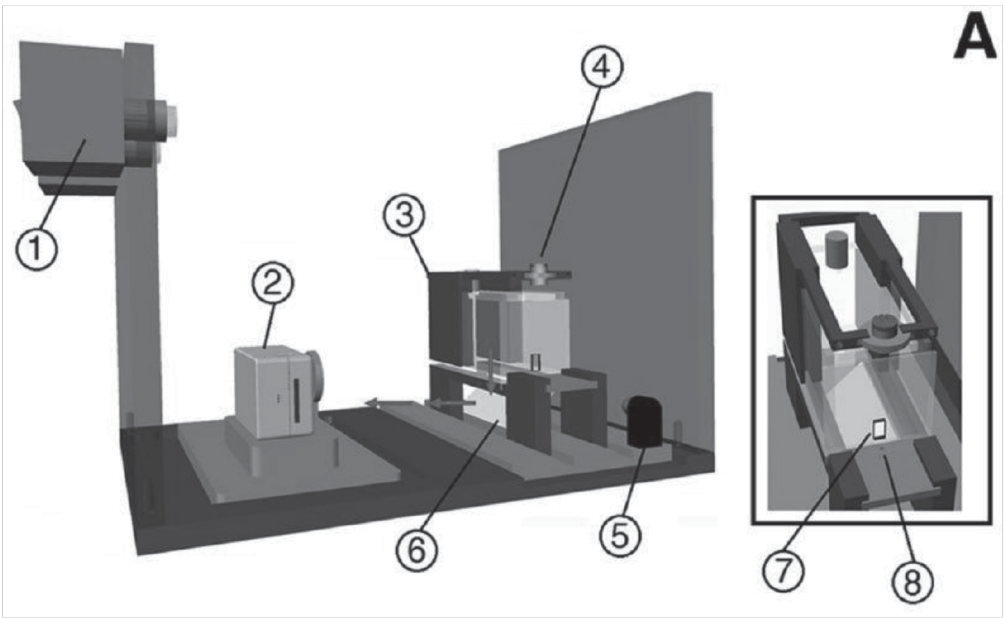

Fig. 4. *Schematic representation of the apparatus, which consists of a cold-light source (1), a digital video camera (2), a testing chamber (3), a photocell (4), a red LED, (5) and a mirror (6). The testing chamber has a rectangular aperture in the front wall (7), through which the paw reaches for a food pellet placed in a slot (8).*

Area (CFA) of the hemisphere contralateral to the trained forelimb, using Endhotelin-1 (ET-1), a potent vasoconstrictor. Anesthetized animals were placed in a stereotaxic frame and the skull was exposed. ET-1 was delivered in 3 sites in the CFA (Tennant et al., 2011). The volume of the lesion was computed 30 days after stroke and was 0.76±0.18mm^3.

Despite the small extent of the lesion, the platform efficiently detected a post-stroke motor deficit, specifically an increase in the t-target and in the number of sub-movements needed to complete the retraction task. Consistently, the mean force exerted significantly decreased. To exclude that the worsening in the performance was not due to a loss in motivation or to an unlearning of the task, we checked the number of total attempts, defined as force peaks not overcoming the static friction threshold. The number of total attempts significantly increased in post-stroke trials showing that animals could recall the task but were impaired to perform it.

Our robotic platform can be used not only for monitoring the forelimb motor performance but also as a training device. Thanks to the low complexity of the task and the low stressing manipulation, it was possible to train animals daily for several sessions following stroke. Thus, we asked whether after the first post-stroke worsening, the training on the robotic platform could restore a nearly normal motor performance. To answer this question we decided to apply an intermediate intensity rehabilitative-protocol by training animals every 2 days. Results after 2 weeks of robotic-mediated therapy showed a significant improvement in parameters automatically extracted by the robotic device. The mean force exerted, as well as the number of attempts, the number of sub-movements and the t-target all returned to baseline, pre-lesion values (Fig.3).

Altogether, these results indicate that our robotic platform allows for quantitative and reliable assessment of pre- and post-stroke forelimb motor function in mice, providing also an innovative rehabilitative approach.

KINEMATIC CHARACTERIZATION OF POST-STROKE REACHING IMPAIRMENTS

As mentioned previously, to objectively evaluate the effectiveness of a rehabilitative therapy, the

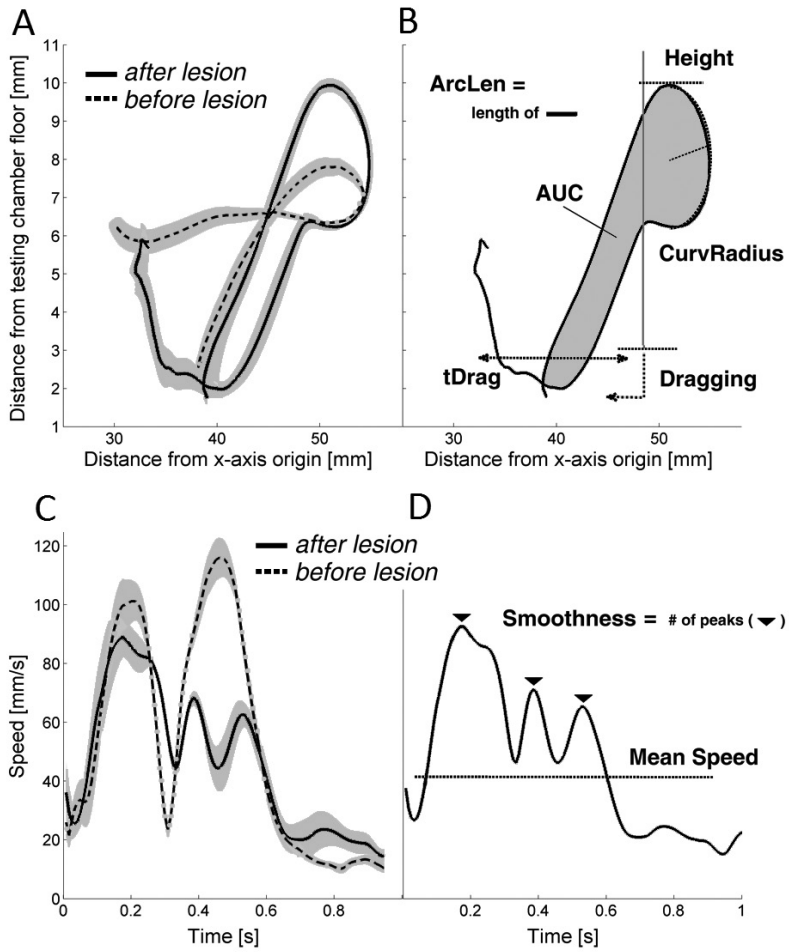

Fig. 5. ***A)*** *Average trajectories (solid lines) recorded before (dotted line) and after stroke (continuous line) during 2 experimental sessions of the same mouse. The standard error is represented by the shaded region.* ***B)*** *Kinematic parameters computed from the trajectories. The vertical line represents the aperture in the front wall.* ***C)*** *Average profiles and standard errors of tangential velocities measured before (dotted line) and after stroke (continuous line).* ***D)*** *Kinematic parameters computed from the speed curves.*

training-induced motor improvement should also be detectable in other motor paradigms not directly related to the exercise task. Concerning animal models, in the literature some motor tests for rodents have been characterized and generally accepted for evaluating post-stroke forelimb motor function (Brooks & Dunnett, 2009). One of the most used motor tests is the Skilled Reaching Task: animals are trained to reach food pellets with their forepaw and to bring it into the mouth without dropping it. The percentage of correct grasps is a relevant end-point measure for the assessment of the forelimb function also during post-stroke recovery (Alaverdashvili & Whishaw, 2010; Klein et al., 2012; Moon et al., 2009; Whishaw et al., 2008). To better distinguish between "true recovery" and compensation, kinematics could provide useful information about the reaching movement strategy by means of the study of the paw trajectory. This kinematic approach has already been used in some reports, but the evaluation phase was always made manually by the experimenter, thus possibly introducing experimenter's bias and dramatically increasing the time required for analysis (Alaverdashvili & Whishaw, 2013; Braun et

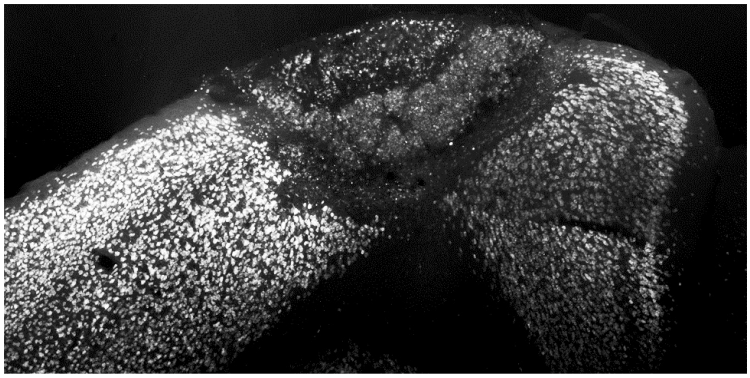

Fig. 6. *Stroke-induced brain damage. Representative coronal brain section showing the lesion and the perilesional area with a NeuN immunostaining.*

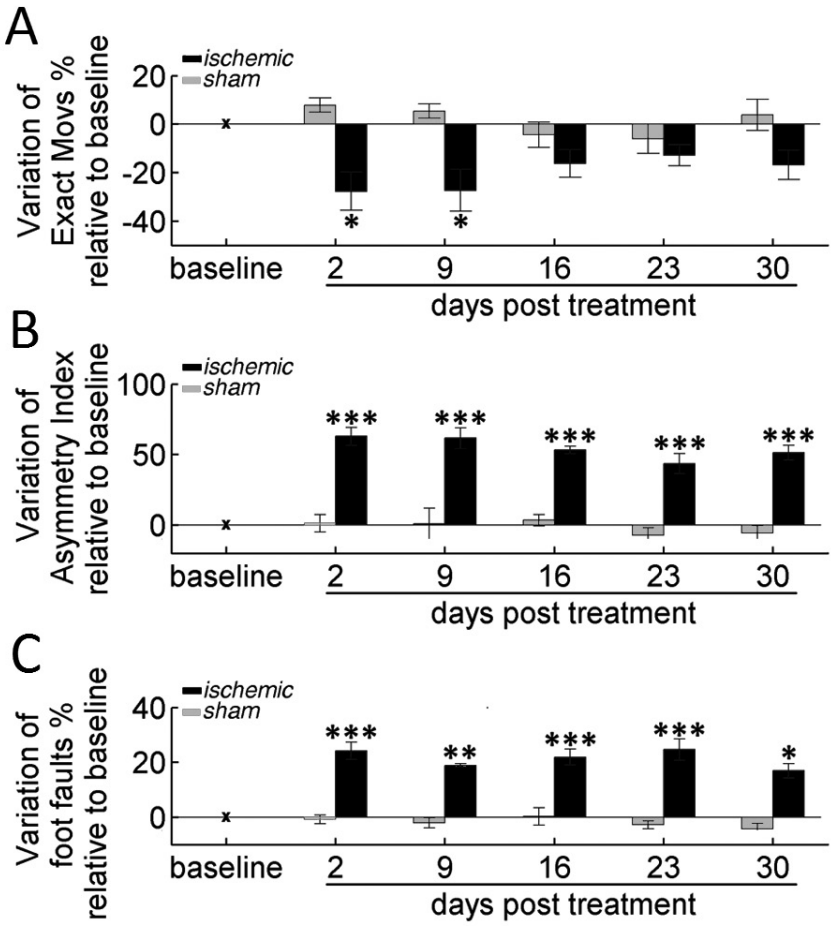

Fig. 7. *End-point measures for assessing forelimb impairments.* ***A)*** *Variation of % Exact Movs in the pellet reaching task.* ***B)*** *Changes in the Asymmetry Index in the Schallert cylinder.* ***C)*** *Modifications in % of Foot Faults in the Gridwalk test. For all panels, bars refer to days 2, 9, 16, 23, and 30 after treatment: stroke (black) or sham (grey). Values are normalized by subtracting baselines, and plotted as means ± standard error. Asterisks correspond to the following significance values: *P < 0.05, **P < 0.01, ***P < 0.001.*

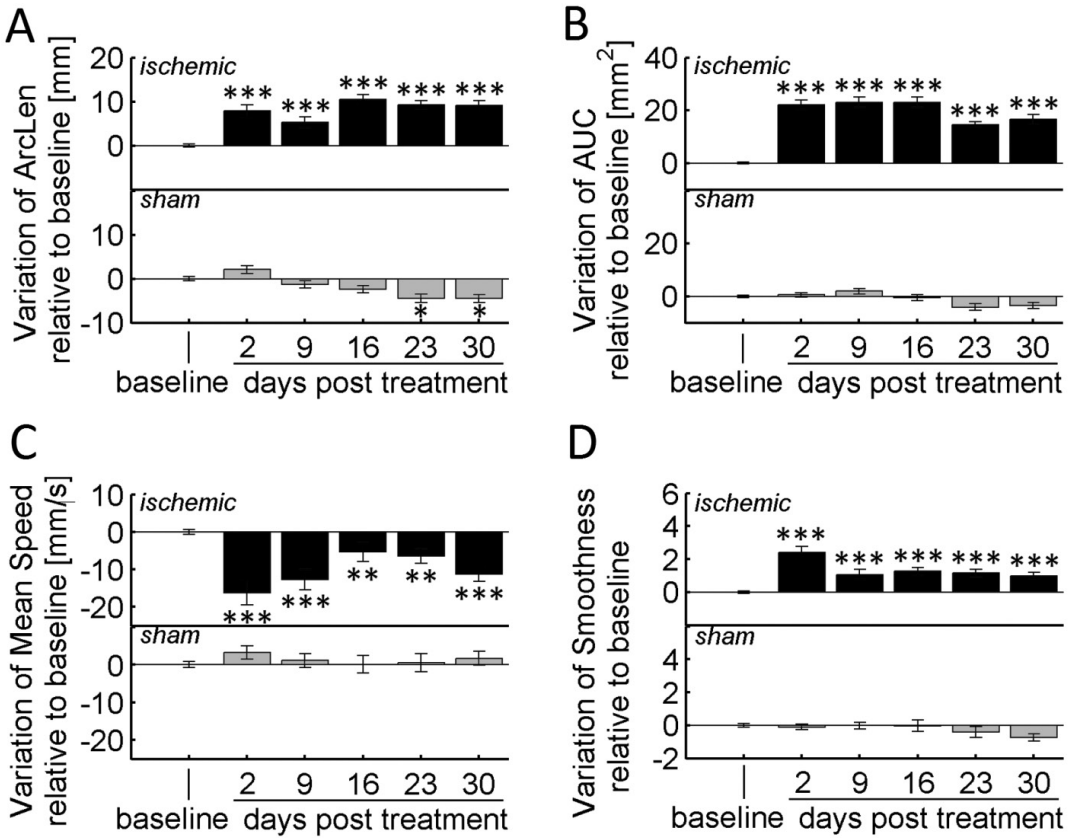

Fig. 8. *Overall kinematic modifications. Variations of (**A**) ArcLen, (**B**) AUC, (**C**) Mean Speed, and (**D**) Smoothness at 2, 9, 16, 23, and 30 days after treatment: stroke (black) or sham (grey). Values are normalized by subtracting baselines and plotted as means ± standard error. Asterisks correspond to the following significance values: *P < 0.05, **P < 0.01, ***P < 0.001.*

al., 2012).

In our recent paper we characterized a semi-automated tool for studying limb kinematics of reaching movements in a phothrombotic mouse model (Lai et al., 2015). We developed an algorithm for tracking paw movements without any markers stuck on the skin. The behavioral task was inspired on the classical Skilled reaching test: during the learning phase (1-2 weeks) animals were trained to reach food pellets with their preferred paw. When the percentage of correct grasps reached a plateau value, we started with the kinematic acquisition in the apparatus. During the acquisition phase, animals were placed in the testing chamber with a rectangular aperture (0.5 x 1.3 cm, 3 mm from the floor) on the frontal wall. During the task mice used this aperture to reach a food pellet, placed in a slot 8 mm distant, with their forepaw. A photo-diode placed under the slot signaled to a photo-detector when the pellet was removed from the slot, i.e. when the mouse grasped the pellet. The reaching movement was recorded by a high-frame rate video camera placed laterally to the testing chamber (Fig. 4). Before testing, the mouse preferred paw was painted with a green non-toxic dye to allow the automated extraction of the paw trajectory. Briefly, the algorithm aligns the photo-cell switching signals with the recorded video and extracts the paw trajectory for each trial by detecting the green pixels, i.e. the paw, in each frame of the video. The algorithm can compute several parameters

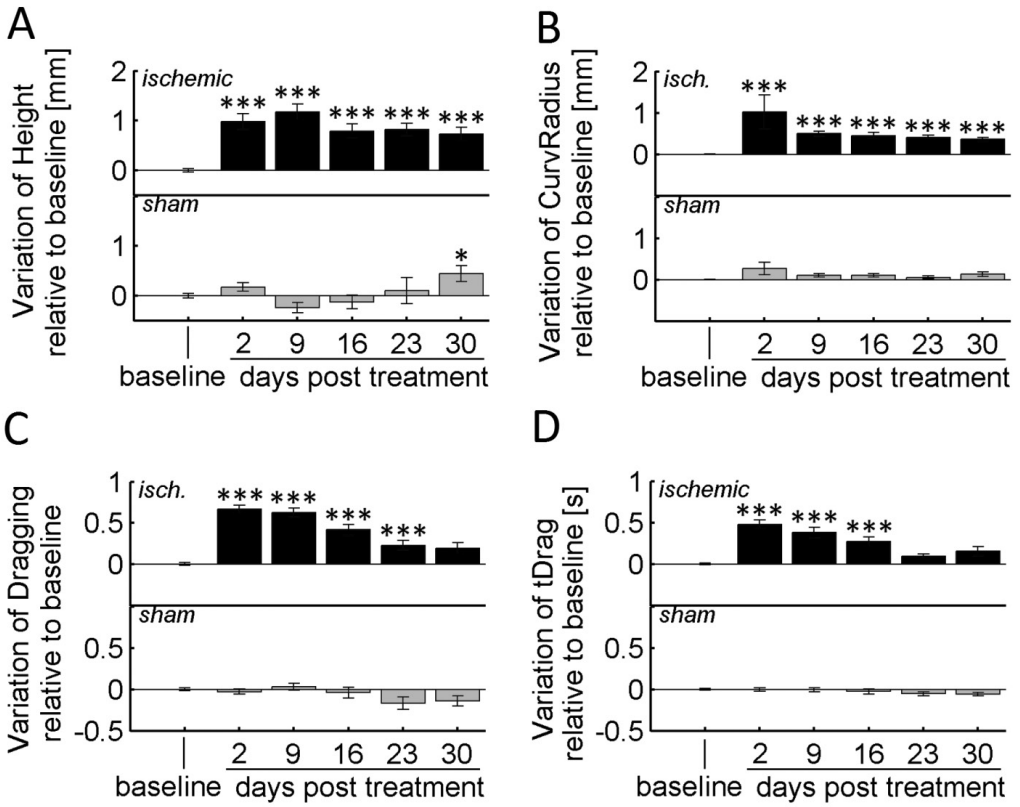

Fig. 9. *Local kinematic modifications. Variation of (**A**) Height, (**B**) CurvRadius, (**C**) Dragging, and (**D**) tDrag at 2, 9, 16, 23, and 30 days after treatment: stroke (black) or sham injection (grey). Values are normalized by subtracting baselines, and plotted as means ± standard error. Asterisks correspond to the following significance values: *P < 0.05, **P < 0.01, ***P < 0.001.*

from the reaching trajectory: length of the end-point trajectory (ArcLen), the area enclosed by the curve (AUC), the average tangential velocity (Mean Speed) and the movement smoothness, quantified by the number of peaks in the tangential velocity profile (Smoothness). Local curve modifications take into account changes in the maximum height reached by the paw during the movement (Height), the curvature of the trajectory when the paw approaches the pellet (CurvRadius), the fraction of the total trials during which a dragging movement occurs (Dragging) and the duration of dragging (tDrag) (Fig. 5). To assess a comparable kinematic analysis among trials, we decided to consider only trajectories of correct grasping movements, with the paw starting on the floor and finishing at the mouth for eating.

To evaluate whether kinematic parameters were affected by an ischemic motor injury, we induced a Rose Bengal-mediated photothrombotic cortical stroke in the Caudal Forelimb Area of the hemisphere contralateral to the preferred paw. After the Rose Bengal i.p. injection (0.2 ml; 10mg/ml), the targeted cortical area (0.5 mm anterior and 1.75 lateral to Bregma) was illuminated through the intact skull for 15 min using a cold light source. The resulting lesion (1.22±0.57 mm^3) had an ischemic core characterized by a completely loss of neuron (NeuN-staining), confined by a surrounding glial scar (Fig. 6). After stroke, animals were tested on the Skilled Reaching test once a week and their performance resulted worsened.

Indeed, we documented a dramatic decrease in the percentage of correct grasps, but after 2 weeks this end-point measure spontaneously recovered. To evaluate the overall motor deficit we measured the end-points also in two classical motor tests: the Gridwalk test and the Schallert Cylinder test. Consistently, we observed a significant increase in the number of contralesional foot faults and a simultaneous shift in the asymmetry index toward the healthy forelimb, respectively. Interestingly, no spontaneous recovery was evident in either of these tests (Fig. 7).

Strikingly, also kinematic parameters were affected by the ischemic injury. Some of these remained affected until 30 days after stroke, such as the Area Under the Curve, the Length of the trajectory path (ArcLen), the Height of the curve, the mean Speed and the Smoothness. Overall, the post-stroke reaching movement resulted chronically wider, slower and less precise (Fig. 8 and Fig. 9A-B). On the contrary, some kinematic parameters, such as the Dragging, spontaneously recovered from the third week after stroke (Fig. 9C-D).

In conclusion, this innovative semi-automated tool is useful for discriminating between motor recovery and spontaneous compensative adjustments.

CONCLUSIONS

Robotic rehabilitation is largely used in clinical procedures, since it provides many advantages in terms of monitoring, intensity and repeatability of the motor rehabilitation. However, mechanisms underlying functional motor recovery after stroke are still unknown. Animal models are particularly suitable for collecting informative behavioral, molecular and electrophysiological data. Moreover, murine models are useful in this context because of their possibility to manipulate genetic factors, using transgenic mice.

The true recovery versus compensation is an important issue to keep in mind. Without any doubt, achieving an improvement in end-point measures is still a good result, even though aiming at a complete recovery is more desirable. The signs of compensative behavior could suggest the presence of a neural substrate to modulate and, possibly, to drive toward a complete motor recovery.

Studying spontaneous neuroplasticity and neural rearrangements after stroke is a crucial point for implementing innovative plasticizing and rehabilitative treatments, as it has been carried out in many recent pre-clinical and clinical papers. The Constraint Induced Movement Therapy (CIMT) is largely used in post-stroke humans and it is considered one of the most effective treatment in physical therapy (Kwakkel et al., 2015). It consists of constraining the non-paretic arm for a prolonged period while forcing the use of the paretic limb. Consistently, studies on rats demonstrated that the forced use of the non-paretic limb is maladaptive for the impaired forelimb (Allred & Jones, 2008; Allred et al., 2010). The balance between inhibition and excitation in perilesional areas is another topic of great interest. Rodent models allow to modulate, for example, the GABAergic system by means of pharmacology, optogenetics or chemogenetics. In mouse studies, the modulation of the tonic GABA system has been tested as post-stroke therapy with positive results (Clarkson et al., 2010).

Our idea is that the robot-mediated rehabilitation could be improved through its association with another plasticizing treatment, targeting and enhancing the spontaneous post-stroke plasticity. To validate the efficacy of these combined therapies, it is important, in humans as well as in mice, to use reliable, quantitative and objective tools that extensively discriminate between “true recovery” and compensation. In addition, to better exploit the animal models advantages and to have the highest translational value, it is critical to use evaluating tools and rehabilitative approaches as comparable as possible to those used in humans. In this perspective, both our papers introduced two useful high-technological instruments to reduce the gap between clinical and pre-clinical studies.

ACKNOWLEDGEMENTS

This work was supported by a grant from Fondazione Pisa. We thank Dr. A. Ghionzoli for providing mechanical support.

REFERENCES

Aisen, ML, HI Krebs, N Hogan, F McDowell, and BT Volpe. (1997) The effect of robot-assisted therapy and

rehabilitative training on motor recovery following stroke. *Arch Neurol* **54**(4): 443–46.

Alaverdashvili, M, and IQ Whishaw. (2010) Compensation aids skilled reaching in aging and in recovery from forelimb motor cortex stroke in the rat. *Neuroscience* **167**(1): 21–30.

Alaverdashvili, M, and IQ Whishaw. (2013) A behavioral method for identifying recovery and compensation: hand use in a preclinical stroke model using the single pellet reaching task. *Neurosci Biobehav Rev* **37**(5): 950–67.

Allred, RP, CH Cappellini, and TA Jones. (2010) The 'good' limb makes the 'bad' limb worse: experience-dependent interhemispheric disruption of functional outcome after cortical infarcts in rats. *Behav Neurosci* **124**(1): 124–32.

Allred, RP, and TA. Jones. (2008) "Maladaptive Effects of Learning with the Less-Affected Forelimb after Focal Cortical Infarcts in Rats." *Exp Neurol* **210**(1): 172–81.

Braun, RG, EM Andrews, and GL Kartje. (2012) Kinematic Analysis of motor recovery with human adult bone marrow-derived somatic cell therapy in a rat model of stroke. *Neurorehabil Neural Repair* **26**(7): 898–906.

Brewer, L, F Horgan, a Hickey, and D Williams. (2013) Stroke rehabilitation: recent advances and future therapies. *QJM* **106**: 11–25.

Brooks, SP, and SB Dunnett. (2009) Tests to assess motor phenotype in mice: a user's guide. *Nat Rev Neurosci* **10**(7): 519–29.

Clarkson, AN, BS Huang, SE Macisaac, I Mody, and ST Carmichael. (2010) Reducing excessive GABA-mediated tonic inhibition promotes functional recovery after stroke. *Nature* **468**(7321): 305–9.

Fasoli, SE, HI Krebs, J Stein, WR Frontera, and N Hogan. (2003) Effects of robotic therapy on motor impairment and recovery in chronic stroke. *Arch Phys Med Rehabil* **84**(4): 477–82.

Ginsberg, MD, and R Busto. (1989) Rodent models of cerebral ischemia. *Stroke* **20**(12): 1627–42.

Kitago, T, J Liang, VS Huang, S Hayes, et al. (2013) Improvement after constraint-induced movement therapy: recovery of normal motor control or task-specific compensation? *Neurorehabil Neural Repair* **27**(2): 99–109.

Klein, A, L-AR Sacrey, IQ Whishaw, and SB Dunnett. (2012) The use of rodent skilled reaching as a translational model for investigating brain damage and disease. *Neurosci Biobehav Rev* **36**(3): 1030–42.

Krebs, HI, and N Hogan. (2006) Therapeutic robotics: a technology push. *Proc IEEE* **94**(9): 1727–37.

Kwakkel, G, JM Veerbeek, EEH van Wegen, and SL Wolf. (2015) Constraint-induced movement therapy after stroke. *Lancet Neurol* **14**(2): 224–34.

Lai, S, A Panarese, C Spalletti, C Alia, et al. (2015) Quantitative kinematic characterization of reaching impairments in mice after a stroke. *Neurorehabil Neural Repair* **29**(4): 382–92.

Moon, SK, M Alaverdashvili, AR Cross, and IQ Whishaw. (2009) Both compensation and recovery of skilled reaching following small photothrombotic stroke to motor cortex in the rat. *Exp Neurol* **218**(1): 145–53.

Posteraro, F, S Mazzoleni, S Aliboni, B Cesqui, et al. (2009) Robot-mediated therapy for paretic upper limb of chronic patients following neurological injury. In *J Rehab Med* **41:** 976–80.

Sacrey, L-AR, M Alaverdashvili, and IQ Whishaw. (2009) Similar hand shaping in reaching-for-food (skilled reaching) in rats and humans provides evidence of homology in release, collection, and manipulation movements. *Behav Brain Res* **204**(1): 153–61.

Sicuri, C, G Porcellini, G Merolla, G Merolla, T Rimini, and L V Beethoven. (2014) Robotics in shoulder rehabilitation. *Muscles Ligaments Tendons J* **4**(2): 207–13.

Spalletti, C, S Lai, M Mainardi, A Panarese, et al. (2014) A robotic system for quantitative assessment and poststroke training of forelimb retraction in mice. *Neurorehabil Neural Repair* **28**(2): 188–96.

Tennant, KA, DL Adkins, NA Donlan, AL Asay, et al. (2011) The organization of the forelimb representation of the C57BL/6 mouse motor cortex as defined by intracortical microstimulation and cytoarchitecture. *Cereb Cortex* **21**(4): 865–76.

Volpe, BT, HI Krebs, N Hogan, L Edelstein OTR, C Diels, and M Aisen. (2000) A novel approach to stroke rehabilitation: robot-aided sensorimotor stimulation. *Neurology* **54**(10): 1938-44.

Whishaw, IQ, P Whishaw, and B Gorny. (2008) The structure of skilled forelimb reaching in the rat: a movement rating scale. *J Vis Exp* (18).

Zangwill, OL. (1947) Psychological aspects of rehabilitation in cases of brain injury. *Br J Psychol Gen Sect* **37**(2): 60–69.

NEUTRALIZATION OF THE SECOND ARGININE ALONG THE S_4 SEGMENT OF Kv7.2 POTASSIUM CHANNEL SUBUNITS PRODUCES GAIN-OF-FUNCTION EFFECTS AND CAUSES EPILEPTIC ENCEPHALOPATHY

M. DE MARIA[1], M.V. SOLDOVIERI[1], F. MICELI[2], P. AMBROSINO[1] and M. TAGLIALATELA[1,2]

[1]Department of Medicine and Health Science, University of Molise, Campobasso, Italy;
[2]Department of Neuroscience, University of Naples "Federico II", Naples, Italy

Mutations in the *KCNQ2* gene, encoding for Kv7.2 voltage-gated K^+ channel subunits underlying the neuronal M-current, have been associated with a wide spectrum of early-onset epileptic disorders ranging from benign familial neonatal seizures to severe epileptic encephalopathy. In the present conference report, we describe our latest results in which, by using mutagenesis, electrophysiology, biochemical, and multistate modeling techniques, the molecular mechanism(s) underlying channel dysfunction caused by mutations affecting the R201 residue of Kv7.2 recently found in patients affected with epileptic encephalopathy (R201C or R201H) have been investigated. Electrophysiological studies revealed that the mutations, affecting the second arginine (R2) in the voltage sensing domain (VSD), destabilized the resting state of the channel, thereby producing gain-of-function effects, opposite to the loss-of-function effects produced by previously found disease-causing mutations. Multistate structural modeling revealed that the R2 residue stabilized the resting state of the VSD by forming an intricate network of electrostatic interactions with neighboring negatively-charged residues (E130 and E140 in S_2, D172 in S_3), a result also confirmed by disulfide trapping experiments. Thus, the Kv7.2 mutations affecting the R2 residue selectively impair the stability of the resting VSD state, favoring channel opening. In conclusion, the results obtained suggest that mutation-induced increase in Kv7.2 function can be responsible for epileptic encephalopathy in humans.

Seizures are among the most common neurological manifestation in the newborn period, with an estimated incidence of 1.8–3.5 per 1,000 live births (Lanska et al., 1995). Neonatal seizures are hard to differentiate from a variety of normal neonatal movements; they are also likely under-diagnosed because they are not always clinically observable, and continuous video electroencephalographic (EEG) monitoring is necessary to establish seizure frequency in neonates (Tavyev Asher and Scaglia, 2012).

One of the most challenging issues in neonatal epileptology is the assessment of the prognostic factors influencing clinical outcome. In fact, the developing brain is particularly susceptible to the potentially severe effects of epilepsy, and epilepsy, especially when refractory to medications, often results in an epileptic encephalopathy (Berg, 2011), characterized by developmental arrest or regression, usually accompanied by concomitant arrest in brain growth. The clinical picture in intractable epilepsy is that of devastating global developmental delay, with

Key words: epileptic encephalopathy, gain-of-function, Kv7.2, multistate structural modeling

Corresponding author: Maurizio Taglialatela, MD PhD
Department of Medicine and Health Science,
University of Molise
Via De Sanctis,
86100 – Campobasso, Italy
Tel.: +39 0874 404851 Fax: +39 0874 404778
e-mail: m.taglialatela@unimol.it

2279-5855 (2015)

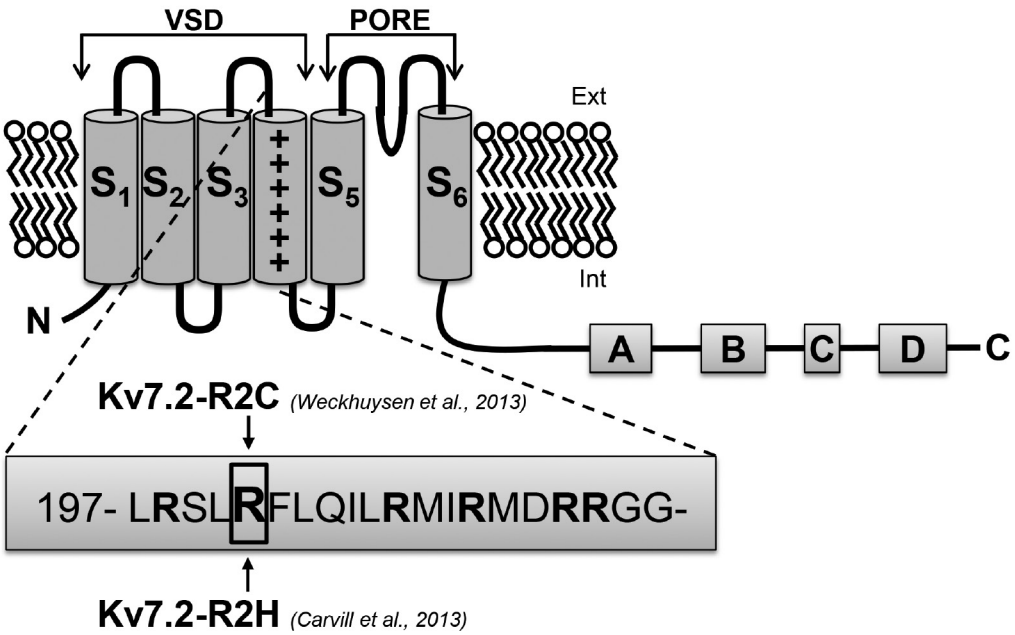

Fig. 1. ***Topology of a Kv7.2 subunit and localization of R2 mutations.*** *Schematic topology of a Kv7.2 subunit with S_1-S_4 transmembrane segments, forming the voltage sensor domain (VSD) and S_5-S_6 segments, forming the pore region. The aminoacid sequence of the S_4 segment is shown: the six arginine residues (R) are in bold; the R2 residue is boxed. EOEE-associated mutations affecting the R2 residue, described in the present paper, are indicated.*

lack of motor, language, social development, visual attention, smiling, and interaction.

Although disease severity in most epileptic patients is likely influenced by largely unknown environmental and genetic risk factors, the wide phenotypic variability of clinical outcome following neonatal seizures is largely recapitulated also in single-gene defects. One paradigmatic example is the *KCNQ2* gene, encoding for voltage-gated potassium (K^+) channel subunits (Kv7.2) which, together with Kv7.3 subunits, contribute to the formation of the M-current (I_{KM}), a widely distributed neuronal K^+ current (Wang et al., 1998). Structurally, all members of the Kv7 family (Kv7.1-Kv7.5) are tetramers of subunits each showing six transmembrane segments (S_1-S_6), and cytoplasmic N- and C-termini of variable length. The pore domain is encompassed by the S_5-S_6 segments and the intervening linker, whereas the transmembrane segments between S_1 and S_4 form the voltage-sensing domain (VSD), with S_4 charged and uncharged residues contributing to voltage-dependent gating (Soldovieri et al., 2007; Miceli et al., 2008; Miceli et al., 2009) (Fig. 1). Mutations in the *KCNQ2* gene are responsible for Benign Familial Neonatal Seizures (BFNS) (Plouin et al., 1994), a rare autosomal-dominant epilepsy of newborn characterized by recurrent seizures that begin in the first weeks of postnatal life and spontaneously remit after few weeks or months (Bievert et al., 1998; Singh et al., 1998). BFNS is characterized by a normal interictal EEG and a benign clinical course, although BFNS individuals show a 10-20-fold higher risk of developing seizures later in life (Plouin et al., 1994).

However, the concept that *KCNQ2* mutations are mostly associated with a benign clinical phenotype was shattered about four years ago, when mostly *de novo* mutations in *KCNQ2* were found in about 10% of patients with unexplained neonatal or early-infantile pharmacoresistant seizures with psychomotor retardation, abnormal EEG, and distinct neuroradiological features, thus defining a so-called "KCNQ2 encephalopathy" (Weckhuysen et al., 2012). Subsequently, *KCNQ2* mutations have also been found in 23% of patients with early onset, severe epilepsies without any familial history of epilepsy (Milh et al., 2013), in 13% of patients

with unexplained neonatal epileptic encephalopathy, with seizure onset in the first month of life and developmental delays (Weckhuysen et al., 2013), and in 0.4% (2/500 cases) of patients affected with a wide clinical range of epileptic encephalopathies (Carvill et al., 2013).

The molecular mechanisms underlying the clinical phenotype in KCNQ2 early-onset epileptic encephalopathy (EOEE) is still matter of debate. Results from studies in which the mutation-induced changes in the functional consequences of Kv7.2 channels have been assessed *in vitro* and in animal models have led to the prevailing hypothesis that most disease-causing mutations produced loss-of-function effects on the channel function. In particular, our group has recently provided the first direct experimental evidence that, in two mutations affecting the distal part of the S_4 domain, the clinical disease severity may be related to the extent of the mutation-induced functional K^+ channel impairment (Miceli et al., 2013), a result confirmed by another study showing that a significant number of EOEE-associated KCNQ2 mutations exert a dominant-negative reduction of the K^+ current (Orhan et al., 2014).

In the present conference report, mutagenesis, electrophysiology, biochemical, and multistate modeling techniques were used to investigate the molecular mechanism(s) underlying disease pathogenesis by newly-identified EOEE-causing mutations affecting the proximal S_4 sequence in Kv7.2 channels (R201C, Weckhuysen et al., 2013; R201H, Carvill et al., 2013).

Homomeric Kv7.2 channels carrying R2 mutations show dramatic gating alterations

The S_4 segment of Kv7 subunits contains six arginine residues separated by two-three uncharged residues; each of this positively-charged residue contributes to voltage-dependent gating of these channels (Miceli et al., 2008). In particular, the second arginine (R201, R2) has been found mutated in two EOEE-affected patients (R2C in Weckhuysen et al., 2013; R2H in Carvill et al., 2013). In particular, in the child carrying the R2C mutation, seizures started on the 2nd day of life; later, the child showed frequent tonic spasm-like seizures, with bursts of erratic myoclonic movements often followed by or intermixed with tonic contractions; she was severely impaired and frequently required oxygen supplementation due to respiratory problems. She died at the age of 2.5 years (Weckhuysen et al., 2013). A similar severe clinical course has also been described for the child carrying the R2H mutation (Carvill et al., 2013).

To investigate the potential functional changes caused by these mutations, wild-type and mutant cDNAs were transiently expressed in Chinese Hamster Ovary (CHO) cells by transient transfection and ~24 h later currents elicited by the encoded channels were recorded by the whole-cell patch-clamp technique. In the first series of experiments, each cDNA was expressed separately, thus giving rise to homomeric channels (either wild-type or mutants). Homomeric wild-type Kv7.2 channels generate K^+ currents characterized by slow time- and voltage-dependent activation kinetics. At the holding voltage of -80 mV, the vast majority of Kv7.2 channels are closed and no currents could be recorded (Fig. 2A). By contrast, homomeric R2C channels showed an almost complete loss of time-dependence in current activation kinetics. While the G/V curve of Kv7.2 channels was sigmoidal, R2C currents showed a mostly linear G/V between +20 mV and -80 mV (Fig. 2A), indicative of a significant loss of voltage-dependent gating; a slight degree of channel deactivation was observed upon membrane hyperpolarization below the holding voltage. The replacement of the same R2 residue with an H (R2H) caused a marked hyperpolarizing shift (about 30 mV) in the voltage-dependence of current activation (Fig. 2A), with a significant fraction of R2H channels being open at -80 mV. Despite such dramatic changes in voltage-dependent gating, all mutant channels retained their K^+ selectivity; in fact, the reversal potential of the currents from Kv7.2 (-79±1 mV), R2C (-79±1 mV), and R2H (-76±1 mV) channels was close to that of a K^+-selective pore (-83 mV under the present recording conditions). Sensitivity to the pore blocker tetraethylammonium (TEA) was also unaffected in both mutant channels, confirming that these mutations do not alter pore structure.

Overall, the data obtained suggest that the mutations herein investigated increased channel sensitivity to voltage, leading therefore to a gain-of-function effect. However, quantitative differences were evident when comparing R2C and R2H channels; in fact, while channels formed by R2C subunits displayed a pronounced loss in voltage-dependent gating, smaller effects were instead observed in R2H

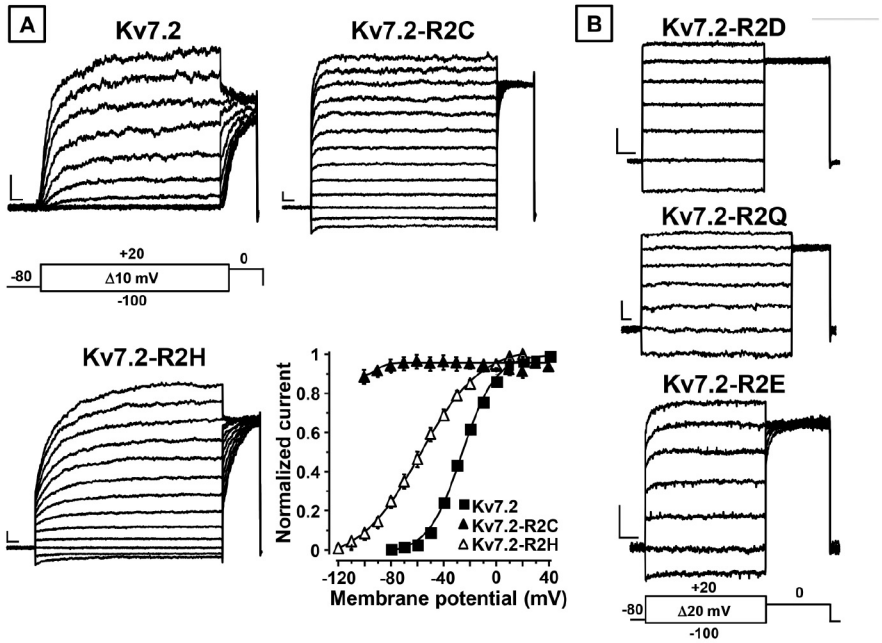

Fig. 2. ***Functional effects of R2 mutations studied in Kv7.2 homomeric channels.*** ***A)*** *Representative current traces recorded in CHO cells expressing wild-type or mutant (R2C, R2H) homomeric Kv7.2 channels. The voltage protocol used for these experiments is shown below the Kv7.2 current traces. Bottom, conductance/voltage curves for the indicated channels. Each data point is the mean±SEM of 7-20 cells recorded in at least three separated experimental sessions.* ***B)*** *Representative current traces recorded in CHO cells expressing R2D, R2Q, R2E homomeric Kv7.2 channels. The voltage protocol used for these experiments is shown at the bottom of current traces.*

channels. The fact that the gating changes of R2H channels were quantitatively smaller than those of R2C channels allows to hypothesize that the removal of the positive charge is in itself responsible for the observed gating alterations; in fact, at physiological pH, histidines are mostly uncharged (pKa is about 6), but a small percentage could be protonated, whereas cysteines, having a pKa of about 8.4, are partly (10%) deprotonated and negatively charged. In keeping with this hypothesis, channels carrying the R2D mutation, similarly to R2Q channels (Miceli et al., 2008), also carried time- and voltage-independent currents (Fig. 2B). Neutralization of the corresponding position in Kv7.1 (Panaghie and Abbott, 2007) or Kv7.4 (Miceli et al., 2012) led to similar gating changes. Single-channel measurements in R2Q channels (Miceli et al., 2008) showed that this mutation affected the conformational changes involving deeper, non-conducting closed states, where most of the voltage-dependent transitions occur (Zagotta and Aldrich, 1990). Noteworthy, a slight difference could be detected between R2D- and R2E-carrying Kv7.2 channels; while a complete loss of both voltage- and time-dependent gating was observed in the first, some time-dependence in the activation could be detected in the latter (Fig. 2B); differences in the side chain length which may allow further electrostatic interactions between the longer E and additional positively charged residues nearby might provide a plausible explanation for this functional heterogeneity.

Gating changes caused by mutant Kv7.2 subunits recorded in heteromeric channels with Kv7.3 subunits

All Kv7.2 mutations have been found in heterozygosity in EOEE-affected patients. To reproduce this genetic balance and considering that I_{KM} is mainly formed upon heteromeric assembly

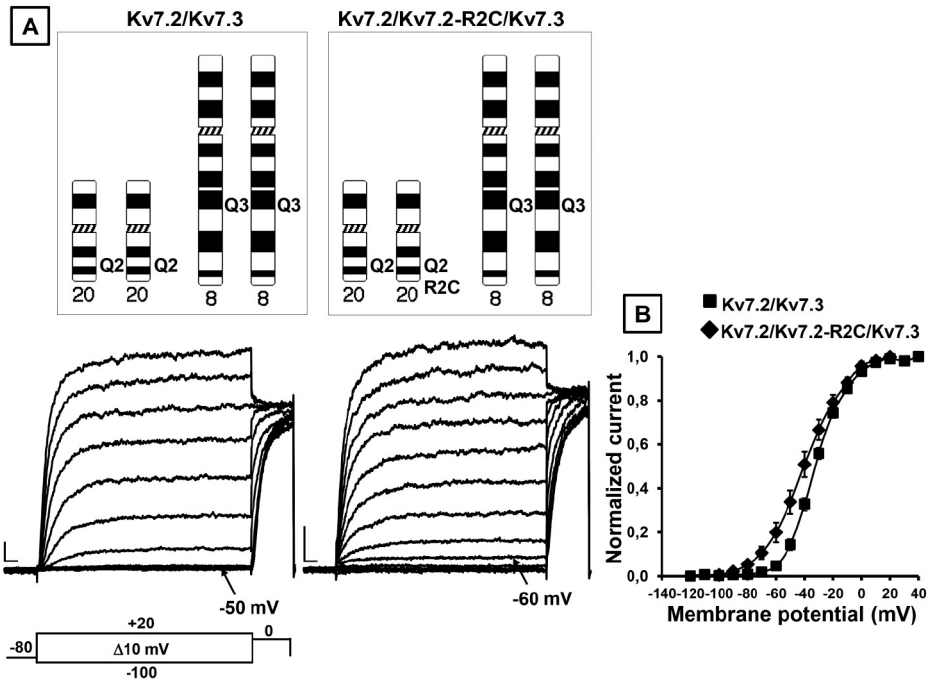

Fig. 3. ***Functional effects of R2 mutations studied in heteromeric channels with Kv7.2 and Kv7.3 subunits. A)*** *Top panel, schematic representation of the genetic balance of a normal individual (left) or of a patient carrying a Kv7.2 mutation in heterozygous condition (right). Bottom panel, representative current traces recorded in CHO cells expressing wild-type (Kv7.2/Kv7.3, left) or mutant (Kv7.2/Kv7.2-R2C/Kv7.3, right) heteromeric channels. The voltage protocol used for these experiments is shown.* ***B)*** *Conductance/voltage curves for the indicated channels. Each data point is the mean±SEM of 6-12 cells recorded in at least three separated experimental sessions.*

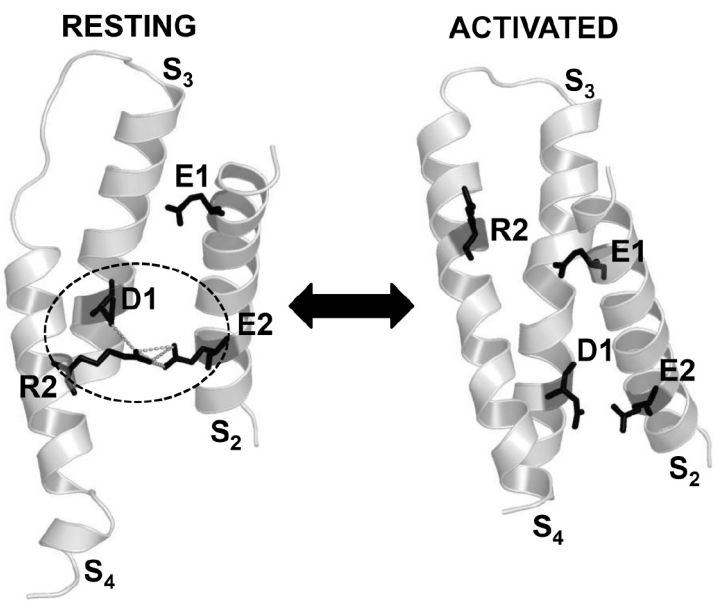

Fig. 4. ***Structural modeling of the VSD of a Kv7.2 subunit.*** *Three-dimensional structural models of the Kv7.2 VSD in the resting (left) or in the activated (right) states. The dashed circle highlights the electrostatic interactions (shown in dashed grey lines) occurring in the resting state between the R201 (R2) residue in the S_4 segment and E140 (E2) in S_2 and D172 (D1) in S_3.*

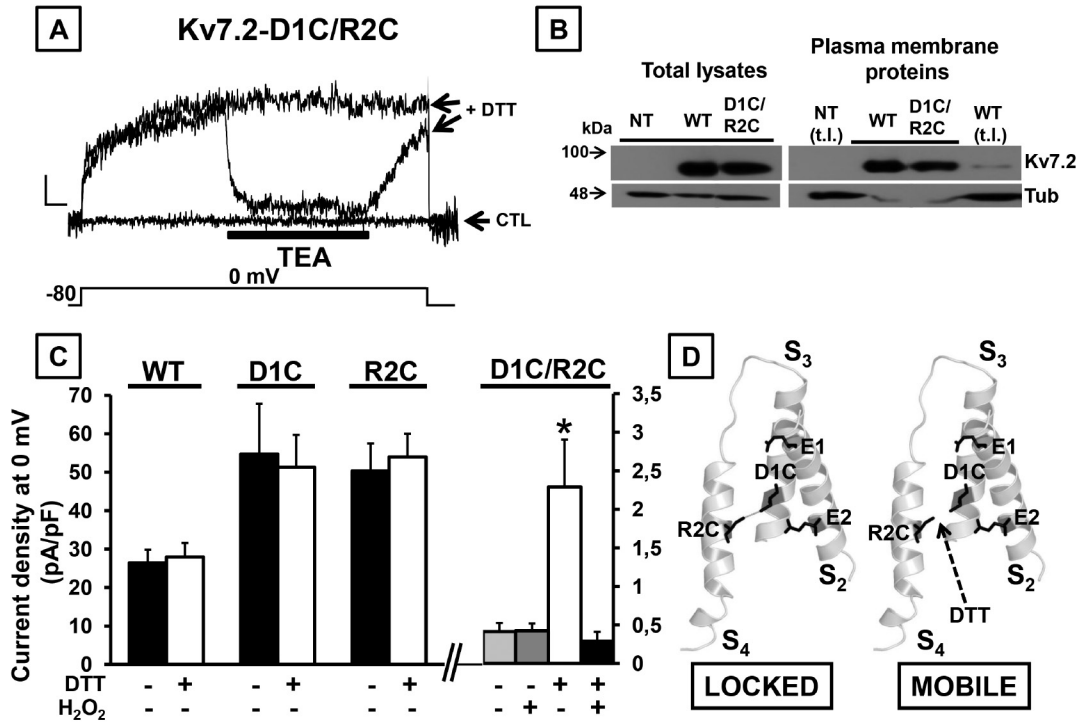

Fig. 5. ***Functional and biochemical characterization of Kv7.2-D1C/R2C channels.*** *A) Superimposed current traces from D1C/R2C channels in control condition (CTL), after pre-incubation with 1 mM DTT before and after perfusion with 3 mM TEA. The bar at the bottom represents the duration of TEA exposure. The voltage protocol used for these experiments is indicated at the bottom of the current traces.* ***B****) Western Blotting analysis performed on total (left) or plasma membrane proteins (right) from untrasfected CHO cells (NT) or from cells expressing wild-type (WT) or D1C/R2C mutant Kv7.2 channels. NT (t.l.) and WT (t.l.) indicate the lanes corresponding to total lysates from NT or Kv7.2 expressing cells, loaded on the same gel together with biotinylated proteins to visualize the molecular mass of Kv7.2 and α-tubulin (Tub). In each panel, the higher and lower blots were probed with anti-Kv7.2, to reveal the protein of interest, and with anti-α-tubulin, to confirm that the biotinylation reagent did not leak into the cell and label intracellular proteins, and to check for equal protein loading.* ***C****) Quantification of current densities of indicated channels in control condition or after treatment with 1 mM DTT and/or 500 mM H_2O_2. *p<0.05, significantly different from the control; n=4-10 cells per group recorded in at least three different experimental sessions.* ***D****) Three-dimensional structural models of the VSD of a D1C/R2C mutant Kv7.2 subunit indicating the presence of a disulfide bridge between D1C and R2C residues in control condition (left), stabilizing the resting state of the VSD (indicated as "locked"), or in the presence of the reducing agent DTT (right) that, disrupting this bond, allows to VSD to be displaced by changes in transmembrane voltage (indicated as "mobile").*

of Kv7.2 and Kv7.3 subunits, we also assessed the functional effects prompted by R2C mutant subunits when expressed simultaneously with Kv7.2 and Kv7.3 subunits. To this aim, we transfected CHO cells with Kv7.2/Kv7.3 cDNAs at 1:1 ratio (to reproduce the genetic status of normal individuals) or with Kv7.2/Kv7.2-R2C/Kv7.3 cDNAs at 0.5:0.5:1 ratio (to reproduce the genetic status of the EOEE-affected patient who carries a single mutant allele) (Fig. 3A). The results obtained show that, when compared to wild-type Kv7.2/Kv7.3 channels, mutant Kv7.2/Kv7.2-R2C/Kv7.3 heteromeric channels show a significant hyperpolarizing shift in the activation gating (Fig. 3B). These results are similar, although less dramatic, than those described for homomeric R2C mutant channels, suggesting that the extent

of the observed alterations are proportional to the number of mutant Kv7.2 subunits expressed.

Structural modeling identifies the molecular basis for the atypical Kv7 gating behavior caused by the R2 mutation

To investigate the molecular mechanisms by which the R2 residue controls gating in Kv7.2 channels, we used multistate molecular modeling to built a three-dimensional model of a single Kv7.2 subunit in different configurations. In particular, we used the coordinates of the six gating states (activated, early deactivated, late deactivated, resting, early activated, and late activated) identified in Kv1.2/2.1 voltage-gated K^+ channels by molecular dynamics simulation (Jensen et al., 2012); this allowed us to follow each residue in Kv7.2 VSD in its interaction with neighboring residues in each of the different structural configurations of the VSD. Interestingly, these models highlighted that, in the resting state, the R2 residue forms strong ionic interactions with negatively-charged residues E140 (E2) in S_2 and D172 (D1) in S_3; such interactions disappear when the VSD is displaced outwardly upon depolarization, to occupy the fully activated state (Fig. 4). Thus, neutralization of the R2 residue would preferentially weaken the network of ionic interactions occurring in the resting state, thereby destabilizing the resting configuration of the VSD and favoring Kv7.2 channel opening.

The interaction between R2 and D1 residues predicted by multistate structural modeling was therefore investigated by disulphide trapping experiments; by this approach, we tested whether the distance between R2 and D1 could allow the formation of a disulphide bond between these residues. To this aim, D1, R2 or both were substituted by cysteine (C) residues, thus obtaining single mutant (D1C or R2C) as well as D1C/R2C double mutant Kv7.2 subunits. The occurrence of a disulphide bond could be hypothesized when the functional properties of channels carrying Cs at both D1 and R2 are different from those of channels carrying C residues at either D1 or R2. Our results suggest that, while single-substituted D1C and R2C channels carried large currents, no measurable current could be detected in double mutant D1C/R2C channels (Fig. 5A). To evaluate whether this lack of current was related to a reduced membrane expression of D1C/R2C double mutant subunits, surface biotinylation experiments in CHO cells expressing either wild-type or double mutant channels were performed. The results obtained indicate that no significant difference could be measured in membrane expression between Kv7.2 and D1C/R2C mutant subunits (Fig. 5B), suggesting that the lack of function of channels formed by D1C/R2C subunits is not due to an altered subunit expression at the plasma membrane. Therefore, we next investigated whether the absence of measurable currents in D1C/R2C channels could be due to the formation of a disulfide bridge between the inserted C residues, which locked the channels in a resting, non-conductive configuration; to this aim, CHO cells expressing D1C/R2C double mutant channels were pre-incubated for 1 h with 1 mM of the reducing agent dithiothreitol (DTT). DTT treatment led to the expression of small, but measurable currents carried by mutant channels (Fig. 5A); application of the oxidant agent hydrogen peroxide (H_2O_2; 500 mM) prevented DTT effects (Fig. 5C). The rescued current was almost fully and reversibly blocked by perfusion with 3 mM TEA (Fig. 5A), suggesting that the DTT-induced currents specifically flowed through Kv7.2 channels. In addition, in wild-type Kv7.2 channels, as well as in D1C and R2C single mutant channels, DTT exposure was ineffective (Fig. 5C). Based on these results, we hypothesize that a disulphide bridge formed between the two cysteine residues inserted at R2 and D1 locks the VSD in the resting state (Fig. 5D, left); such disulphide bond could not be broken by membrane depolarization, but could be at least partially reduced by DTT treatment, therefore recovering the mobility of the VSD during voltage-sensing (Fig. 5D, right). Given that side chains thiols can form disulfide bonds when the distance between their Cβ atoms reaches ~4.6 Å, these data provide functional evidence for the occurrence of an ionized hydrogen bond between D172 and R201 residues stabilizing the resting state of the VSD in native Kv7.2 channels.

CONCLUSIONS

In the present conference report, the functional consequences prompted by recently-described epileptogenic mutations affecting the R2 residue

located in the S_4 transmembrane region of the VDS of Kv7.2 channels have been described. The results obtained, extensively reported in Miceli and coll. (2015), suggest that, opposed to all other mutations investigated to date, Kv7.2 channels carrying either R2C or R2H mutations display an increased (rather than a decreased) stabilization of the open/activated state of the channel voltage sensor. In other words, the VSD of these mutant channels preferentially occupy an activated configuration, thereby allowing significant K^+ ion flow at rather negative membrane voltages in Kv7.2 channels carrying each mutation. These functional effects appear more dramatic in homomeric mutant channels than in heteromeric channels with wild-type Kv7.2 and Kv7.3 subunits, suggesting therefore that the extent of functional changes are proportional to the number of mutant subunits incorporated. Multistate structural modeling and disulfide trapping experiments provided evidence that the R2 residue is involved in electrostatic interactions with neighboring negatively-charged residues present in S_2 and S_3 segments (particularly with the D172 residue). Such network of electrostatic interactions is preferentially formed when the VSD occupies the resting state, whereas it loosens when the VSD is displaced outwardly during channel activation. Therefore, it seems reasonable to conclude that the EOEE-causing mutations affecting the R2 residue in Kv7.2 channels selectively impair the stability of the resting VSD state, without hampering that of the activated state, a result consistent with the described functional changes.

DISCUSSION AND FUTURE PROSPECTIVE

The main conclusion highlighted by the present observations and described in this conference report is that *de novo* mutations found in EOEE patients enhance Kv7.2 channel function by favoring channel opening. Additional EOEE-causing mutations in Kv7.2 VSD (R144Q; Allen et al., 2013) or involving the same R2 residue in Kv7.3 (R230C; Rauch et al., 2012; Allen et al., 2013) also prompted similar functional changes (Miceli et al., 2015). These results have never been reported for Kv7.2 and Kv7.3 channels, where only loss-of-function effects appear to be induced by disease-causing mutations; however, it should be remembered that gain-of-function effects have been described for mutations in other K^+ channels associated with epileptic disorders, such as Kv10.2 (Yang et al., 2013), Kv1.2 (Syrbe et al., 2015), or KCNT1 (Barcia et al., 2012).

One puzzling issue raised by the present results is how to reconcile a gain-of-function mechanism with neuronal hyperexcitability, given the well-known inhibitory function played by subthreshold K^+ channels on neuronal excitability (Wang et al., 1998). Several possible hypotheses can be put forward to attempt to explain this apparent counterintuitive result, including, among others, an increase in Na^+ channel reactivation (Du et al., 2005), the activation of hyperpolarization-activated non-selective cation current I_h (Robinson and Siegelbaum, 2003), and a selective effect on inhibitory neurons (Zemankovics et al., 2010). To address this intriguing issue, we modelled an inhibitory microcircuit between interneurons and pyramidal cells, incorporating the experimentally-defined values of the M-current obtained from Kv7.2/Kv7.3 or by Kv7.2/Kv7.2-R2C/Kv7.3 mutant channels. The results obtained suggest that the presence of R2C mutant subunits depresses interneuron activity, therefore resulting in an effective disinhibition of principal cells (Miceli et al., 2015). Experimental studies in neuronal cells, where mutation-induced changes in other parameters (such as subcellular localization) could also be evaluated, will be needed to confirm such a hypothesis.

For all genetic diseases, the identification of genotype-phenotype correlations which may significantly affect disease prognosis and therapy is among the most challenging issue. This is of particular interest in Kv7.2-related diseases, given the recent approval of retigabine, a selective Kv7.2-5 activator, for the treatment of partial epilepsy resistant to other anticonvulsants (Stafstrom et al., 2011). It seems reasonable to speculate that retigabine might improve Kv7.2 function in the presence of loss-of-function EOEE-associated mutations (Miceli et al., 2013; Orhan et al., 2014); however, retigabine may be ineffective or even detrimental in patients carrying gain-of-function mutations, as those discussed in the present report (R2C or R2H). Thus, *in-vitro* studies, by uncovering disease pathogenetic mechanisms of Kv7.2-related disorders, may be of considerable predictive value for choosing patient-tailored therapeutic strategies with Kv7.2 modulators.

ACKNOWLEDGEMENTS

The authors thank Dr. Thomas J. Jentsch, Department of Physiology and Pathology of Ion Transport, Leibniz-Institut für Molekulare Pharmakologie, Berlin for sharing Kv7.2 and Kv7.3 cDNAs; and Dr. David E. Shaw, D.E. Shaw Research, New York, for providing the coordinates of the six states of the Kv1.2/2.1 chimeric channel. The work described was supported by grants from Telethon (GGP07125), the Fondazione San Paolo-IMI (Project Neuroscience), Regione Molise (Convenzione AIFA/ Regione Molise), the Science and Technology Council of the Province of Avellino, and the Italian Ministry of Education and Research to M.T.

F.M. and M.V.S. are supported by postdoctoral fellowships from the Fondazione Umberto Veronesi and the Italian Society for Pharmacology, respectively.

REFERENCES

Allen AS, Berkovic SF, Cossette P, Delanty N et al. and Winawer MR (2013) De novo mutations in epileptic encephalopathies. *Nature* **501**: 217–221.

Barcia G, Fleming MR, Deligniere A, Gazula VR et al. and Nabbout R (2012) De novo gain-of-function KCNT1 channel mutations cause malignant migrating partial seizures of infancy. *Nat Genet* **44**: 1255–1259.

Berg AT (2011) Epilepsy, cognition, and behavior: The clinical picture. *Epilepsia* 52 Suppl 1:7-12.

Biervert C, Schroeder BC, Kubisch C, Berkovic SF, Propping P, Jentsch TJ, Steinlein OK (1998) A potassium channel mutation in neonatal human epilepsy. *Science* **279**: 403-406.

Carvill GL, Heavin SB, Yendle SC, McMahon JM et al. and Mefford HC (2013) Targeted resequencing in epileptic encephalopathies identifies de novo mutations in CHD2 and SYNGAP1. *Nature Genet* **45**: 825-830.

Du W, Bautista JF, Yang H, Diez-Sampedro A et al. and Wang QK (2005) Calcium-sensitive potassium channelopathy in human epilepsy and paroxysmal movement disorder. *Nat Genet* **37**(7): 733-738.

Jensen MØ, Jogini V, Borhani DW, Leffler AE, Dror RO, Shaw DE (2012) Mechanism of voltage gating in potassium channels. *Science* **336**(6078): 229-233.

Lanska MJ, Lanska DJ, Baumann RJ, Kryscio RJ (1995) A population-based study of neonatal seizures in Fayette County, Kentucky. *Neurology* **45**: 724-732.

Miceli F, Soldovieri MV, Hernandez CC, Shapiro MS, Annunziato L, Taglialatela M (2008) Gating consequences of charge neutralization of arginine residues in the S4 segment of Kv7.2, an epilepsy-linked K^+ channel subunit. *Biophys J* **95**: 2254–2264.

Miceli F, Soldovieri MV, Lugli L, Bellini G et al. and Taglialatela M (2009) Neutralization of a unique, negatively-charged residue in the voltage sensor of Kv7.2 subunits in a sporadic case of benign familial neonatal seizures. *Neurobiol Dis* **34**(3): 501-510.

Miceli F, Vargas E, Bezanilla F, Taglialatela M (2012) Gating currents from Kv7 channels carrying neuronal hyperexcitability mutations in the voltage-sensing domain. *Biophys J* **102**(6): 1372-1382.

Miceli F, Soldovieri MV, Ambrosino P, Barrese V, Migliore M, Cilio MR, Taglialatela M (2013) Genotype–phenotype correlations in neonatal epilepsies caused by mutations in the voltage sensor of Kv7.2 potassium channel subunits. *Proc Natl Acad Sci U S A* **110**(11): 4386–4391.

Miceli F, Soldovieri MV, Ambrosino P, De Maria M, Migliore M, Migliore R, Taglialatela M (2015) Early-onset epileptic encephalopathy caused by gain-of-function mutations in the voltage sensor of Kv7.2 and Kv7.3 potassium channel subunits. *J Neuroscience* **35**(9): 3782–3793.

Milh M, Boutry-Kryza N, Sutera-Sardo J, Mignot C et al. and Laurent Villard (2013) Similar early characteristics but variable neurological outcome of patients with a de novo mutation of *KCNQ2*. *Orphanet J Rare Dis* **8**:80.

Orhan G, Bock M, Schepers D, Ilina EI et al. and Maljevic S (2014). Dominant-negative effects of KCNQ2 mutations are associated with epileptic encephalopathy. *Ann Neurol* **75**(3): 382-394.

Panaghie G, Abbott GW (2007) The role of S4 charges in voltage-dependent and voltage-independent KCNQ1 potassium channel complexes. *J Gen Physiol* **129**(2): 121-133.

Plouin P (1994) Benign familial neonatal convulsions.

In idiopathic generalized epilepsies: clinical, experimental and genetic aspects, edited by Malafosse A, Hirsch E, Marescaux C, Broglin D, Bernasconi R. London: John Libbey, p. 39–44.

Rauch A, Wieczorek D, Graf E, Wieland T et al. and Strom TM (2012) Range of genetic mutations associated with severe non-syndromic sporadic intellectual disability: an exome sequencing study. *Lancet* **380**: 1674–1682.

Robinson RB, Siegelbaum SA (2003) Hyperpolarization-activated cation currents: from molecules to physiological function. *Annu Rev Physiol* **65**: 453-480.

Singh NA, Charlier C, Stauffer D, DuPont BR et al. and Leppert M (1998) A novel potassium channel gene, KCNQ2 is mutated in a inherited epilepsy of newborns. *Nat Genet* **18**: 25-29.

Soldovieri MV, Cilio MR, Miceli F, Bellini G et al. and Taglialatela M (2007) Atypical gating of M-type potassium channels conferred by mutations in uncharged residues in the S_4 region of KCNQ2 causing benign familial neonatal convulsions *J Neurosci* **27**(18): 4919-4928.

Stafstrom CE, Grippon S, Kirkpatrick P (2011) Ezogabine (retigabine) *Nat Rev Drug Discov* **10**(10): 729-730.

Syrbe S, Hedrich UB, Riesch E, Djémié, Lemke JR (2015) De novo loss- or gain-of-function mutations in KCNA2 cause epileptic encephalopathy. *Nat Genet* **47**(4): 393-399.

Tavyev Asher YJ, Scaglia F (2012) Molecular bases and clinical spectrum of early infantile epileptic encephalopathies. *Eur J Med Genet* **55**(5): 299-306.

Wang HS, Pan Z, Shi W, Brown BS et al. and McKinnon D (1998) KCNQ2 and KCNQ3 potassium channel subunits: molecular correlates of the M-channel. *Science* **282**: 1890–1893.

Weckhuysen S, Mandelstam S, Suls A, Audenaert D et al. and de Jonghe P (2012) KCNQ2 encephalopathy: emerging phenotype of a neonatal epileptic encephalopathy. *Ann Neurol* **71**(1): 15-25.

Weckhuysen S, Ivanovic V, Hendrickx R, Van Coster R et al. and De Jonghe P (2013). Extending the KCNQ2 encephalopathy spectrum: clinical and neuroimaging findings in 17 patients. *Neurology* **81**(19): 1697-1703.

Yang Y, Vasylyev DV, Dib-Hajj F, Veeramah KR, Hammer MF, Dib-Hajj SD, Waxman SG (2013) Multistate structural modeling and voltage-clamp analysis of epilepsy/autism mutation Kv10.2-R327H demonstrate the role of this residue in stabilizing the channel closed state. *J Neurosci* **33**: 16586–16593.

Zagotta WN, Aldrich RW (1990) Voltage-dependent gating of Shaker A-type potassium channels in *Drosophila* muscle. *J Gen Physiol* **95**: 29–60.

Zemankovics R, Káli S, Paulsen O, Freund TF, Hájos N (2010) Differences in subthreshold resonance of hippocampal pyramidal cells and interneurons: the role of h-current and passive membrane characteristics. *J Physiol* **588**: 2109-2132.